

Dongtingnoids A–G: Fusicoccane Diterpenoids from a
Penicillium sp.

Qiong Bie,^{†,§} Chunmei Chen,^{†,§} Muyuan Yu,[†] Jieru Guo,[‡] Jianping Wang,[†] Junjun Liu,[†]
Yuan Zhou,[†] Hucheng Zhu,^{*,†} Yonghui Zhang^{*,†}

[†]Hubei Key Laboratory of Natural Medicinal Chemistry and Resource Evaluation,
School of Pharmacy, Tongji Medical College, Huazhong University of Science and
Technology, Wuhan 430030, People's Republic of China

[‡]Department of Pharmacy, Tongji Hospital, Tongji Medical College, Huazhong
University of Science and Technology, Wuhan 430030, People's Republic of China

Corresponding Authors' E-mails:

zhangyh@mails.tjmu.edu.cn. (Y. Z.); zhuhucheng@hust.edu.cn (H.Z.)

[§]These authors contributed equally.

CONTENTS

Table S1. Seed germination-promoting activities of compounds 1 , 4 , 5 , and 8	1
Figure S1. Experimental and calculated ECD spectra of 2-5 and 7	1
Figure S2. Gas Chromatography analyses of compounds 1-5 and 8	2
Figure S3. Key NOESY correlations of compounds 3-5 and 7	3
Spectra of dongtingnoid A (1).....	4
Spectra of dongtingnoid B (2).....	8
Spectra of dongtingnoid C (3).....	13
Spectra of dongtingnoid D (4).....	17
Spectra of dongtingnoid E (5).....	22
Spectra of dongtingnoid F (6).....	26
Spectra of dongtingnoid G (7).....	31
ECD calculations.....	36

Table S1. Seed germination-promoting activities of compounds 1, 4, 5, and 8.

Compounds	First group	Second group	Third group	Germination (%)
1	2	2	2	20
4	2	2	2	20
5	3	3	3	30
8 (Cotylenin E)	3	3	3	30
Water	1	0	0	0

Germination of *Monochoria vaginalis* seeds in water and compounds (50 ppm) in the dark under nonflooded conditions for 13 days. The experiments were repeated for three times.

Figure S1. Experimental and calculated ECD spectra of 2-5 and 7

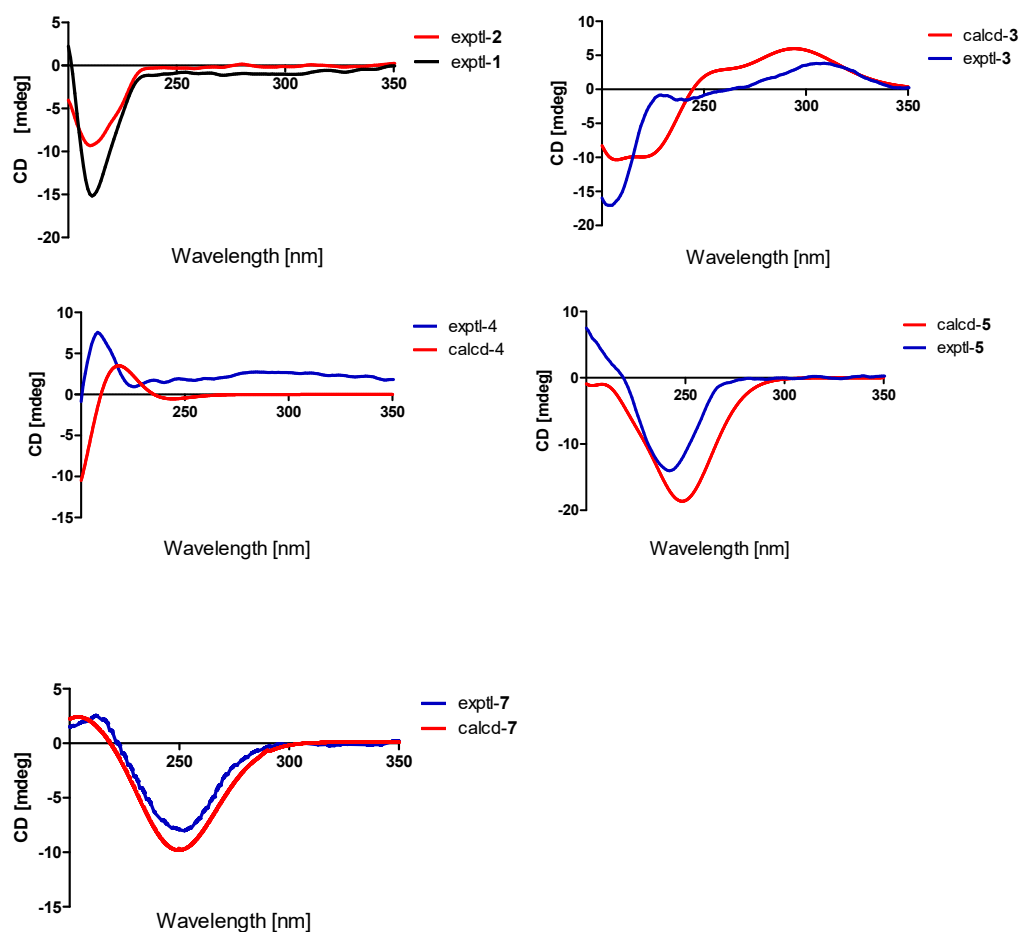
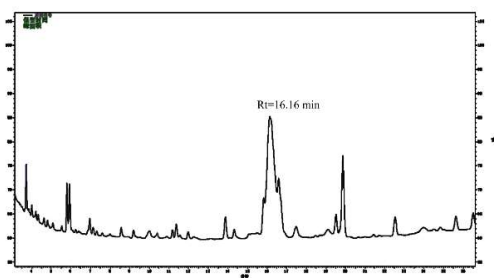
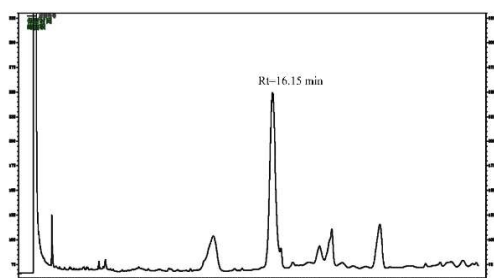


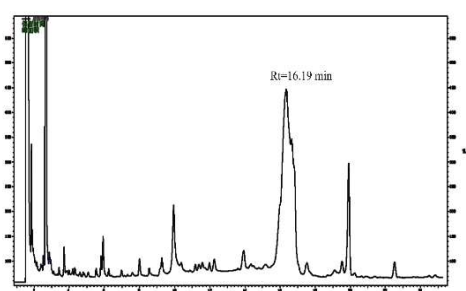
Figure S2. Gas Chromatography analyses of compounds 1-5 and 8



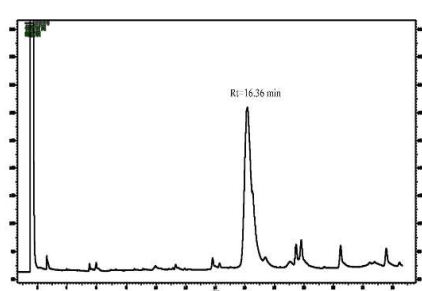
1



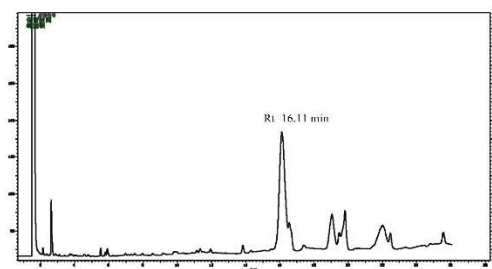
2



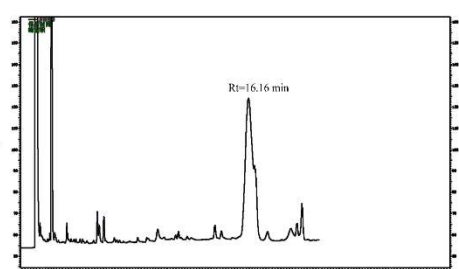
3



4



5



8

Figure S3. Key NOESY correlations of compounds 3-5 and 7

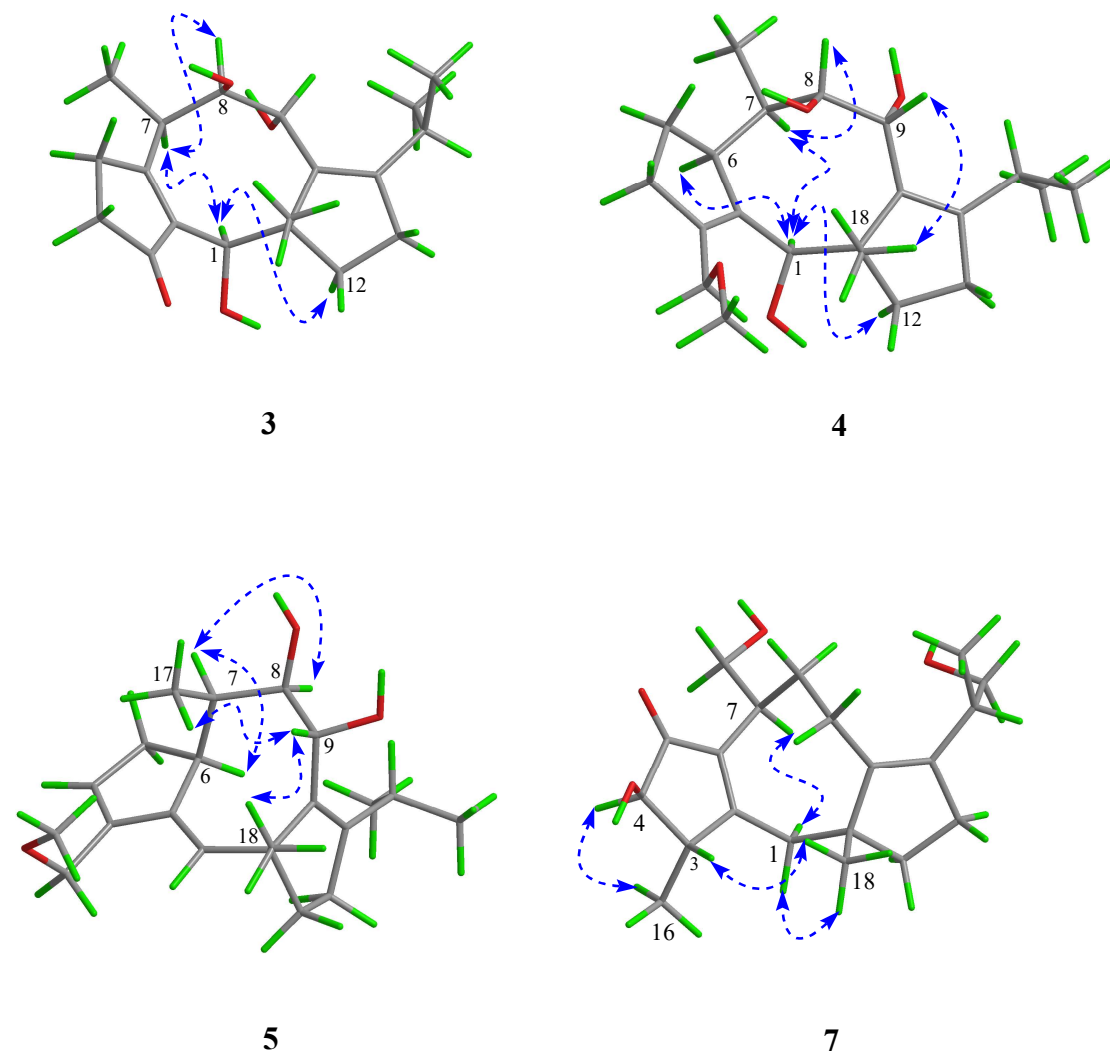


Figure S4. HRESIMS spectrum of dongtingnoid A (1)

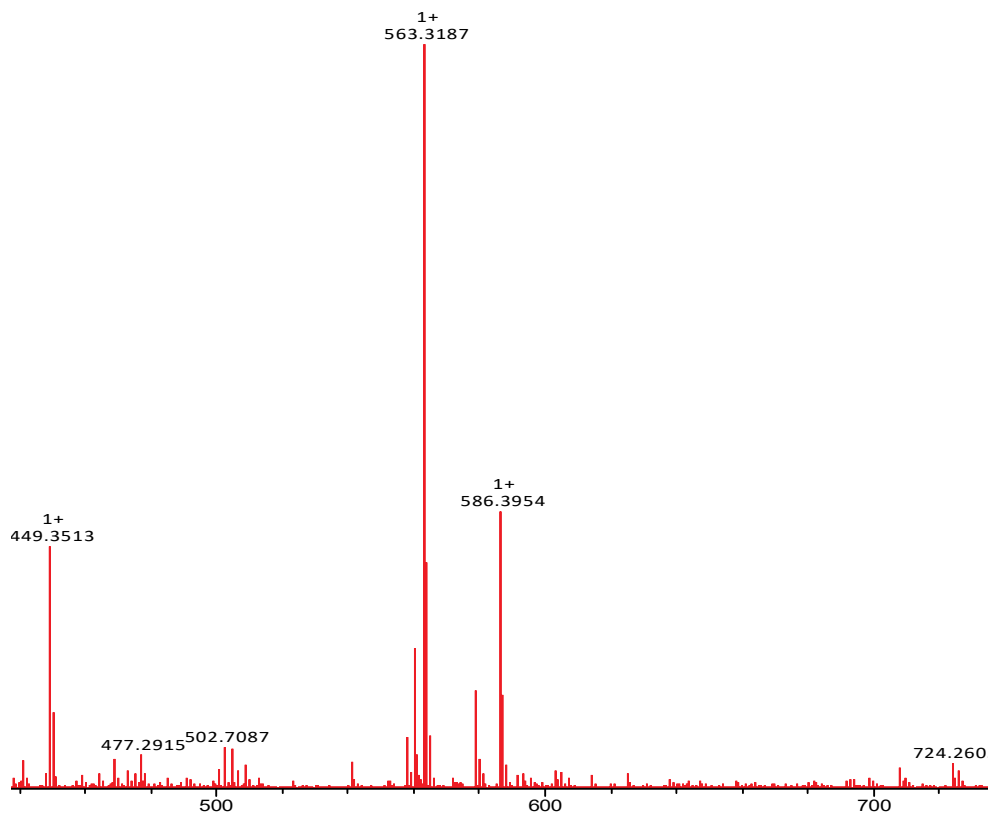


Figure S5. ¹H NMR spectrum of dongtingnoid A (1) in CDCl₃

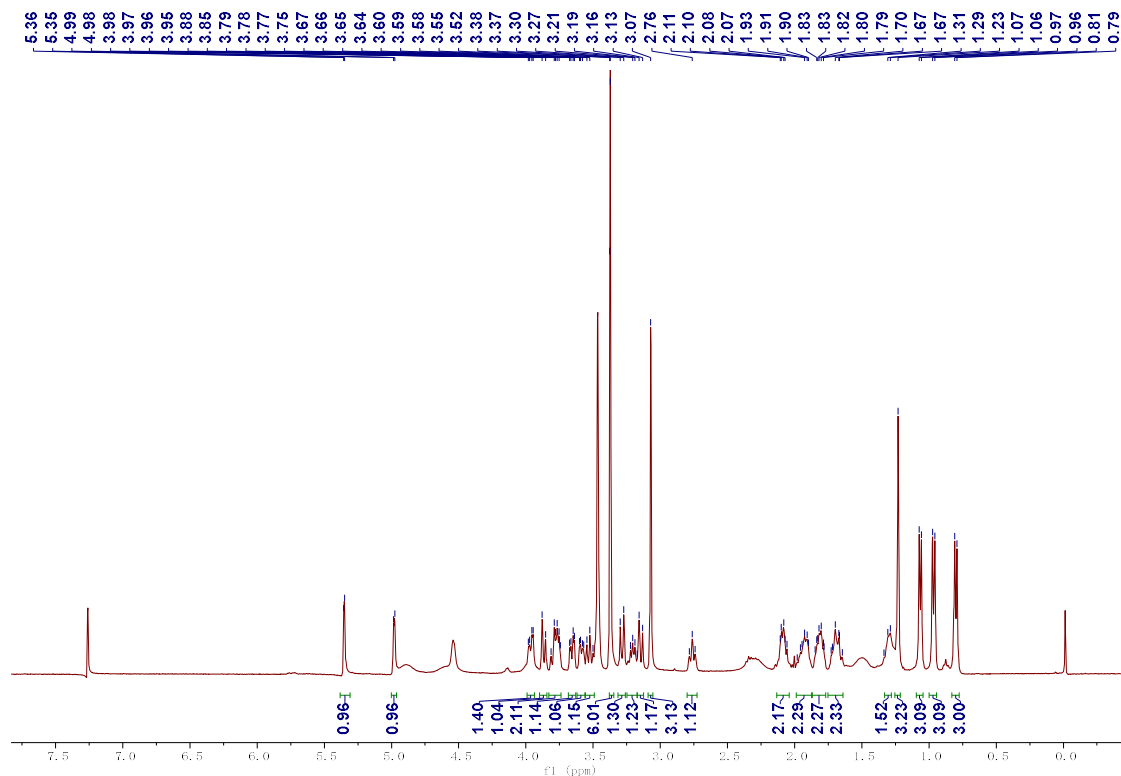


Figure S6. ^{13}C NMR spectrum of dongtingnoid A (**1**) in CDCl_3

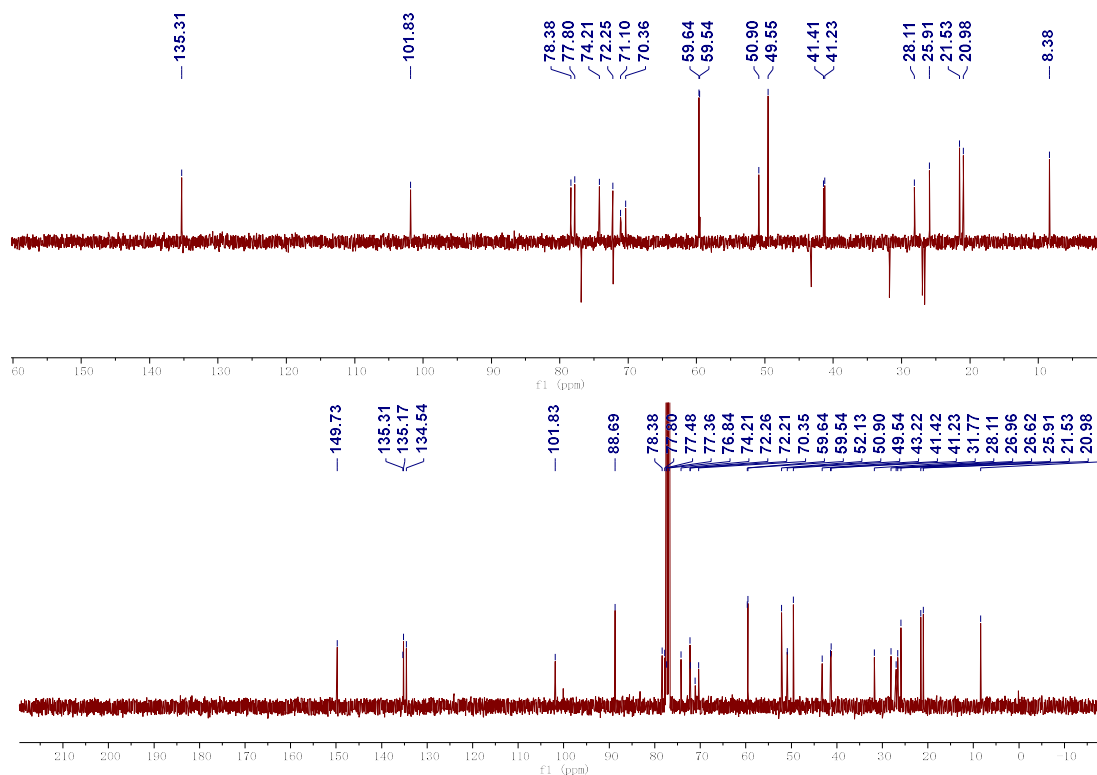


Figure S7. HSQC spectrum of dongtingnoid A (**1**) in CDCl_3

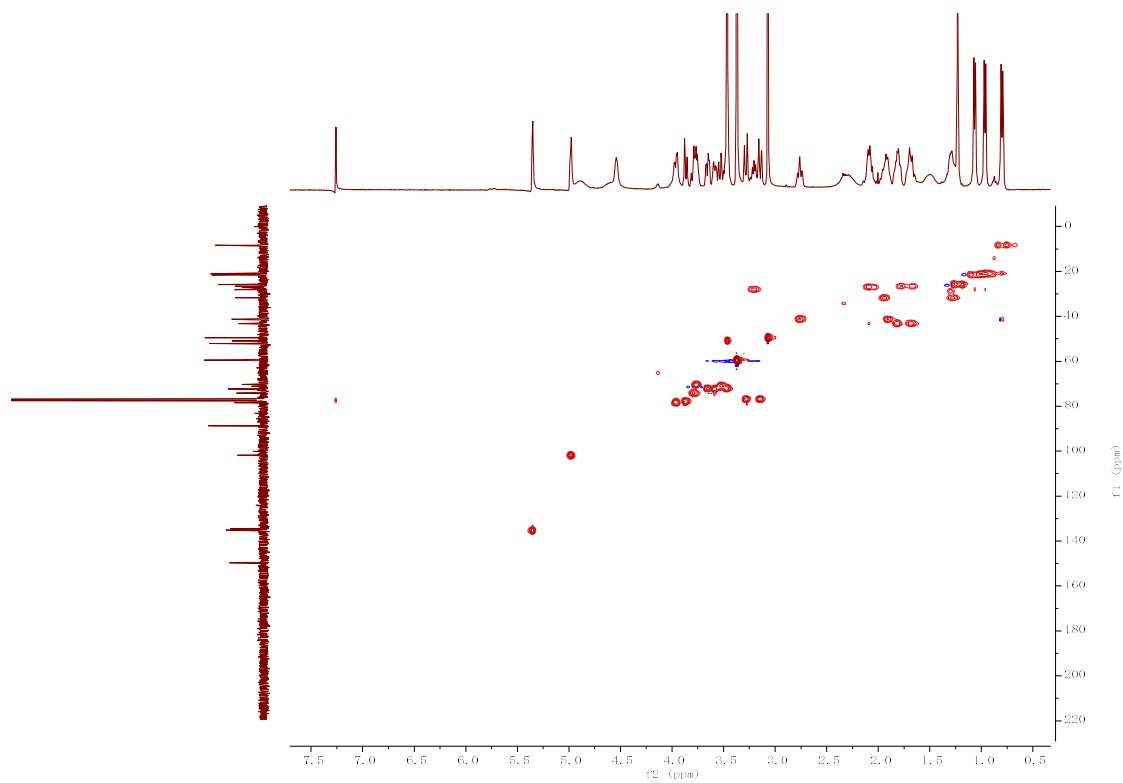


Figure S8. HMBC spectrum of dongtingnoid A (**1**) in CDCl₃

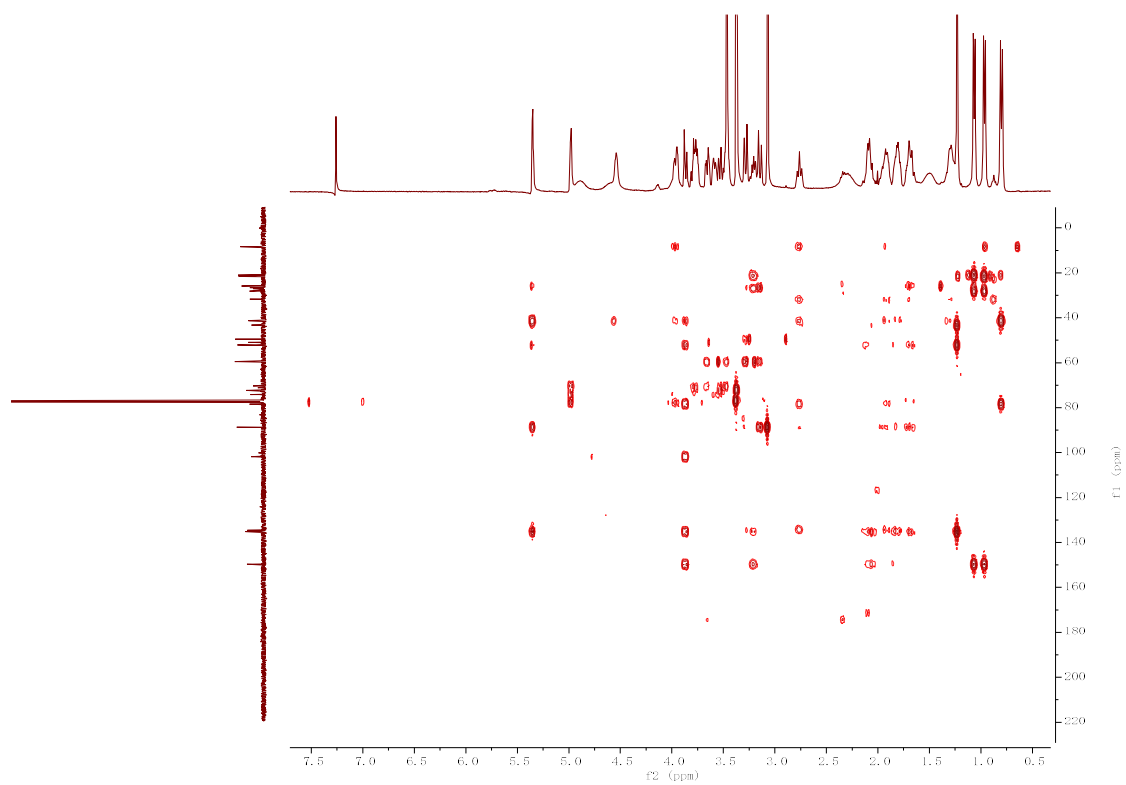


Figure S9. ¹H-¹H COSY spectrum of dongtingnoid A (**1**) in CDCl₃

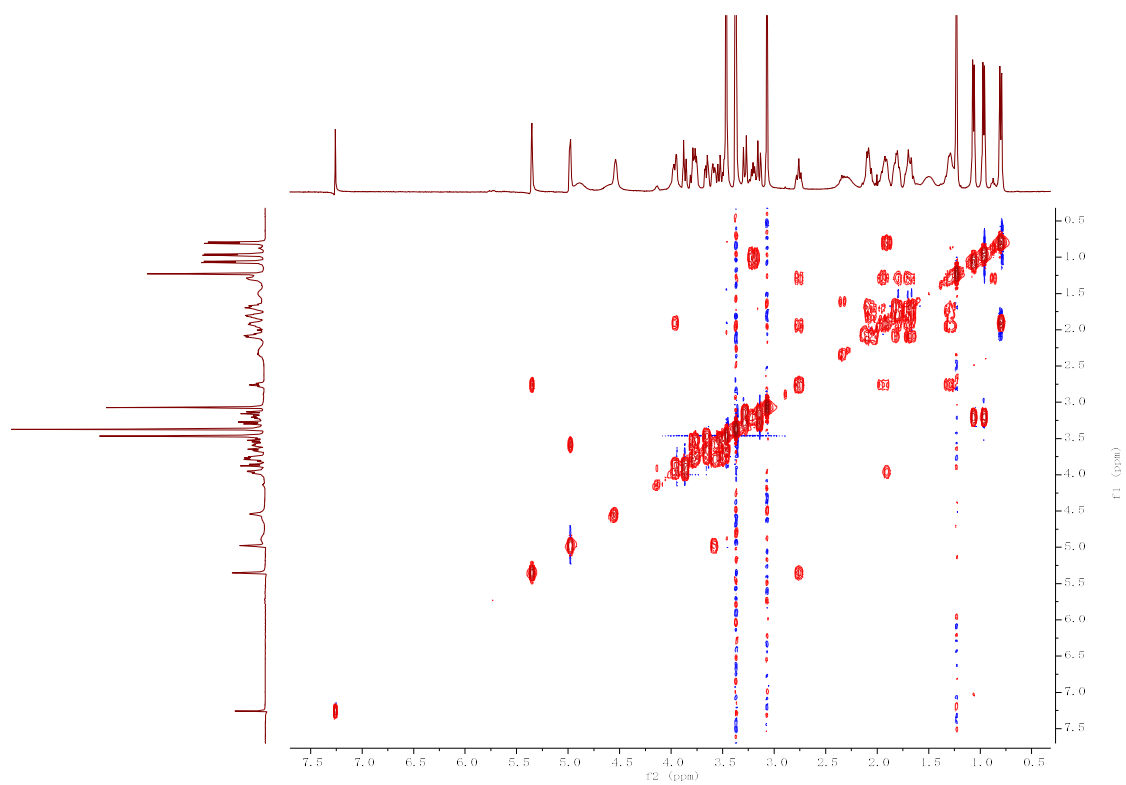


Figure S10. NOESY spectrum of dongtingnoid A (**1**) in CDCl₃

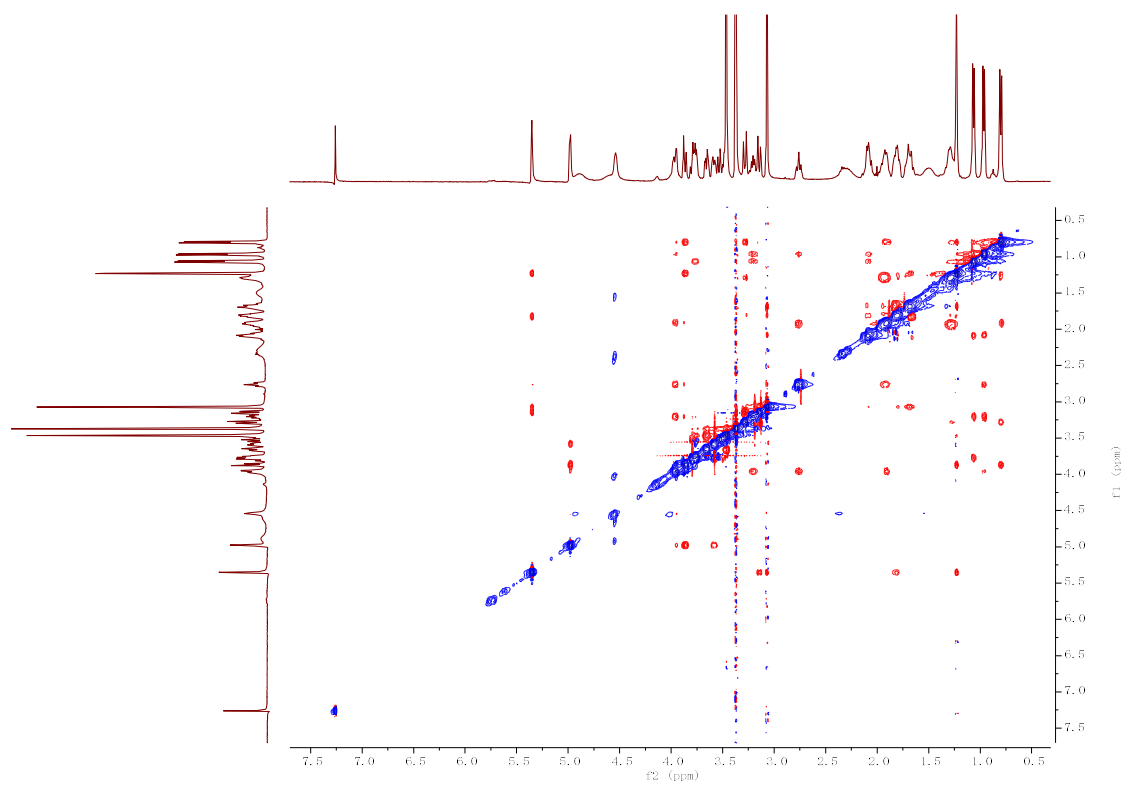


Figure S11. IR spectrum of dongtingnoid A (**1**)

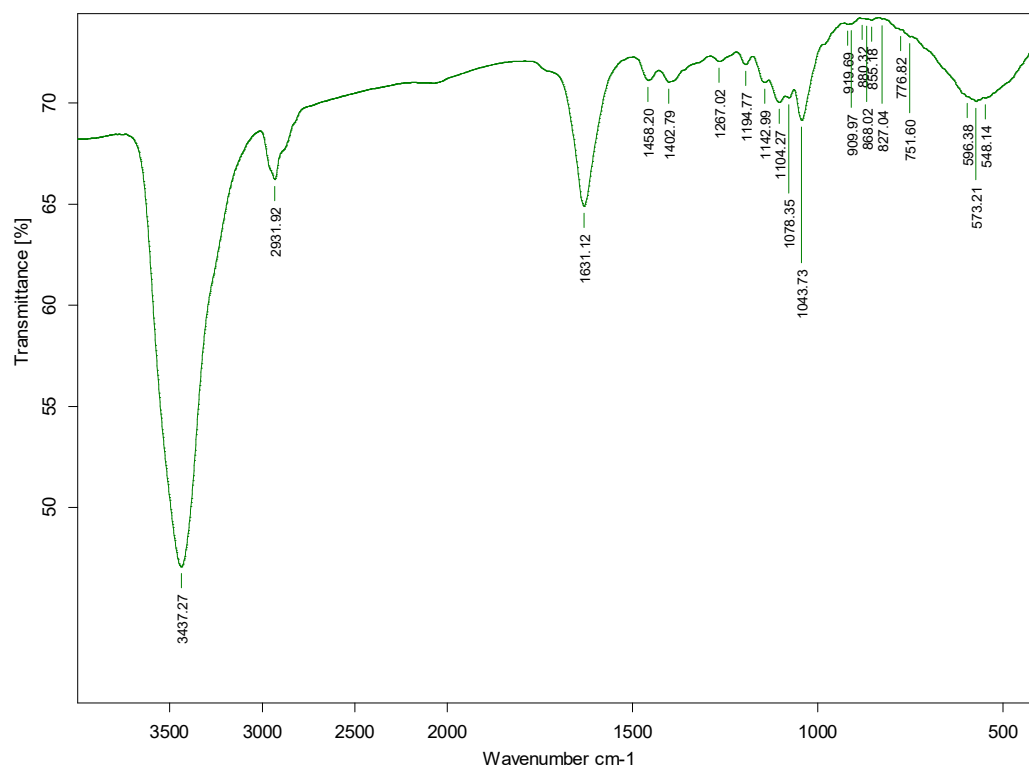


Figure S12. UV spectrum of dongtingnoid A (1)

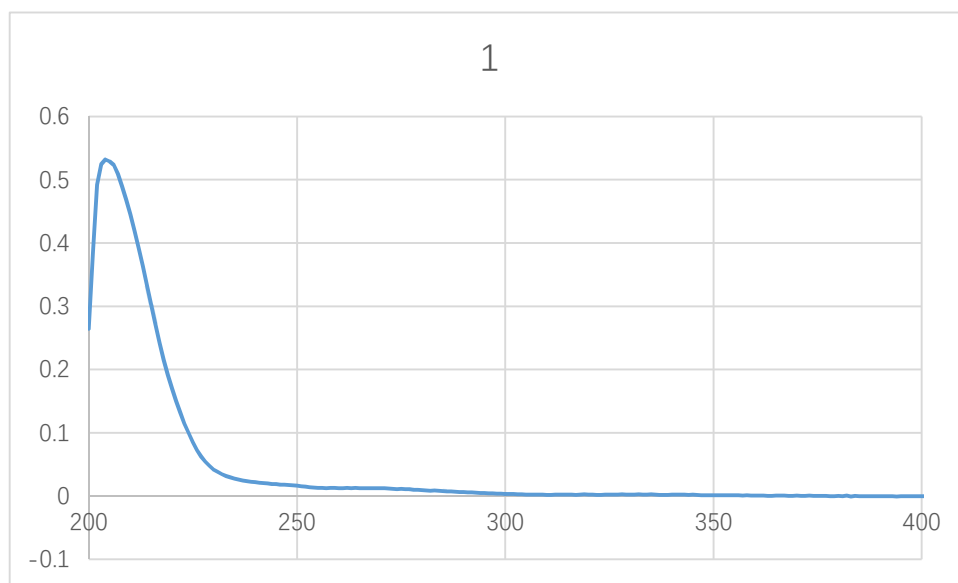


Figure S13. HRESIMS spectrum of dongtingnoid B (2)

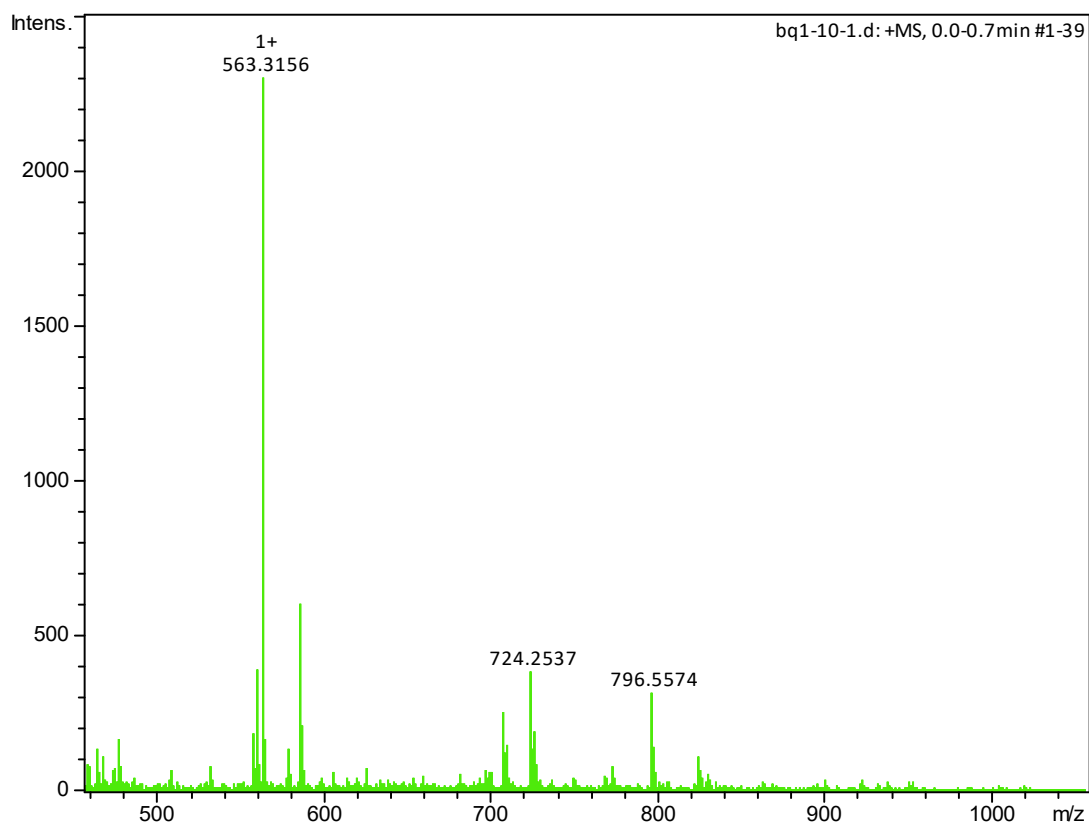


Figure S14. ^1H NMR spectrum of dongtingnoid B (**2**) in CDCl_3

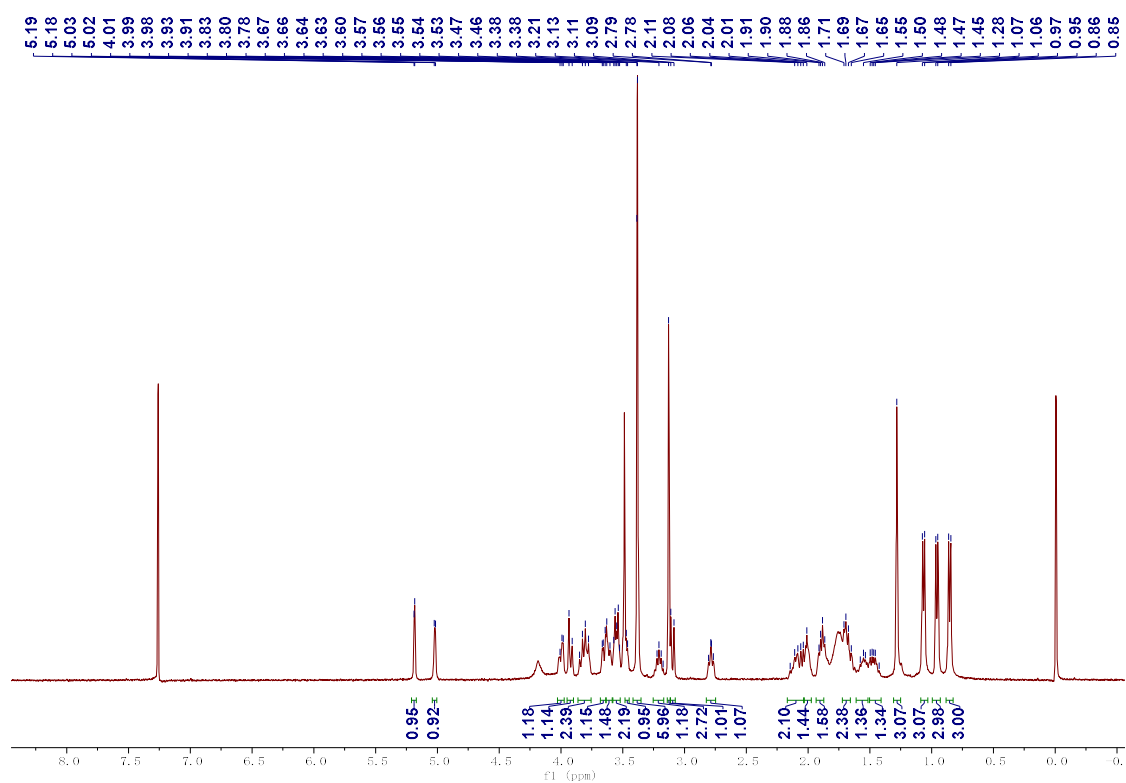


Figure S15. ^{13}C NMR spectrum of dongtingnoid B (**2**) in CDCl_3

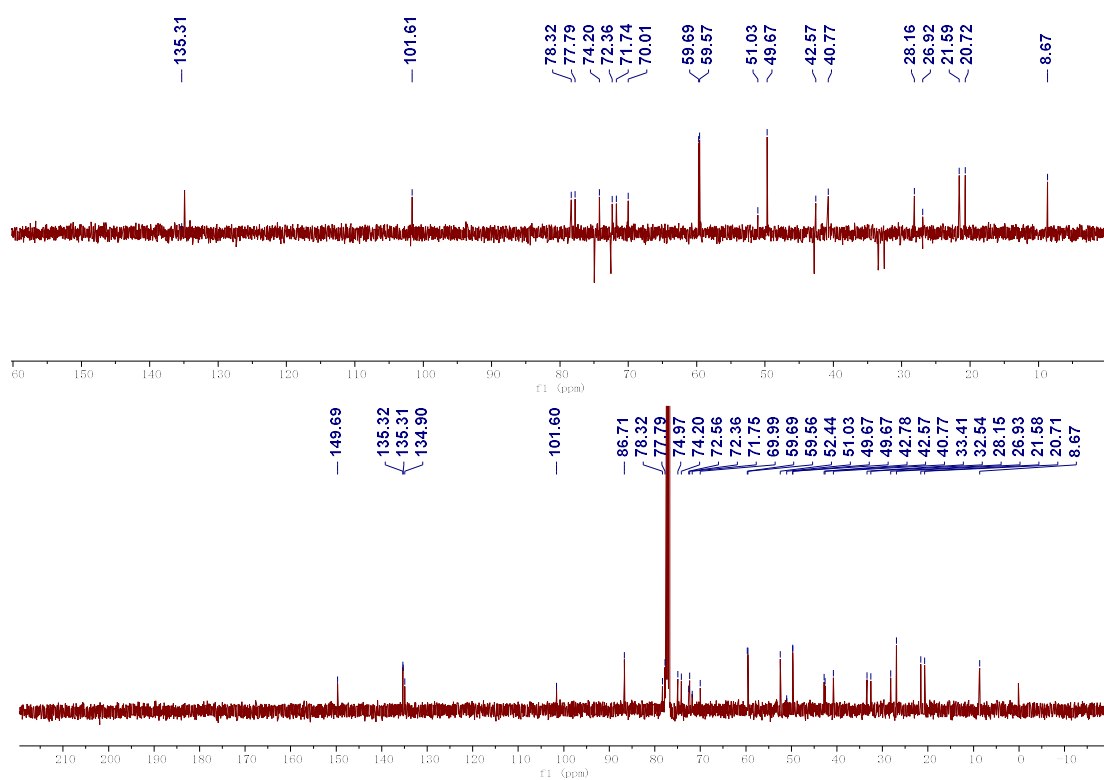


Figure S16. HSQC spectrum of dongtingnoid B (**2**) in CDCl₃

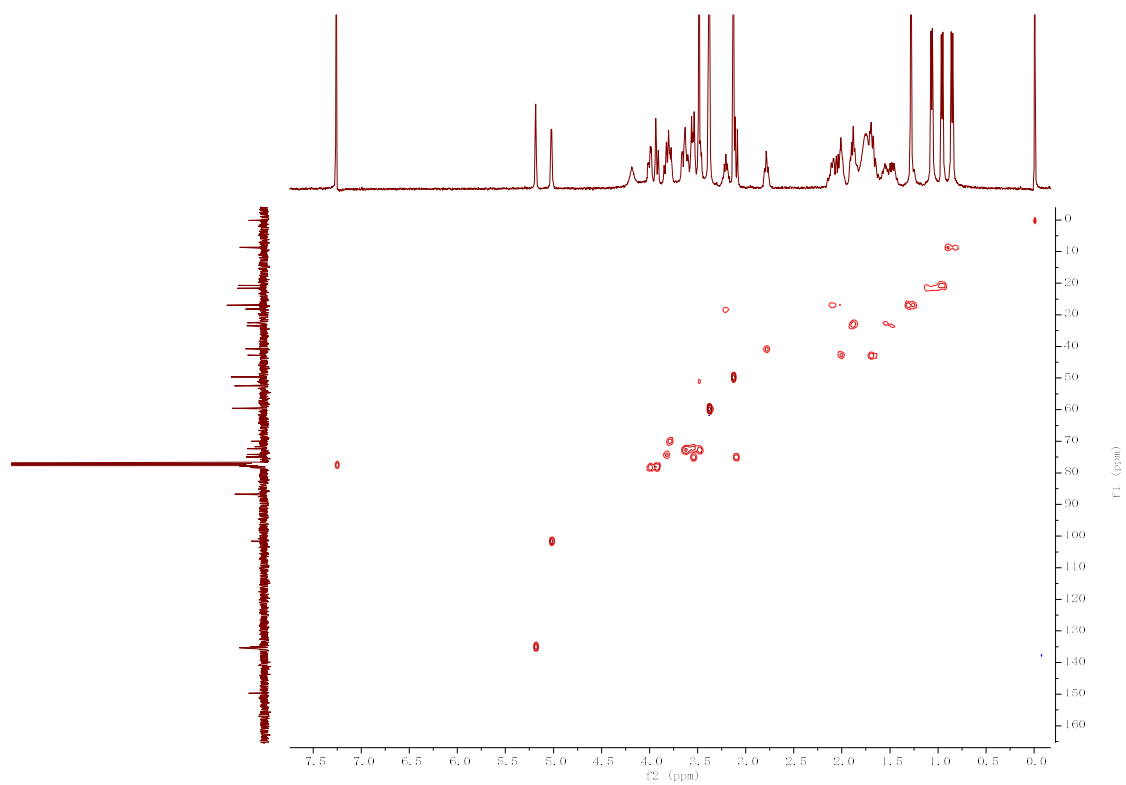


Figure S17. HMBC spectrum of dongtingnoid B (**2**) in CDCl₃

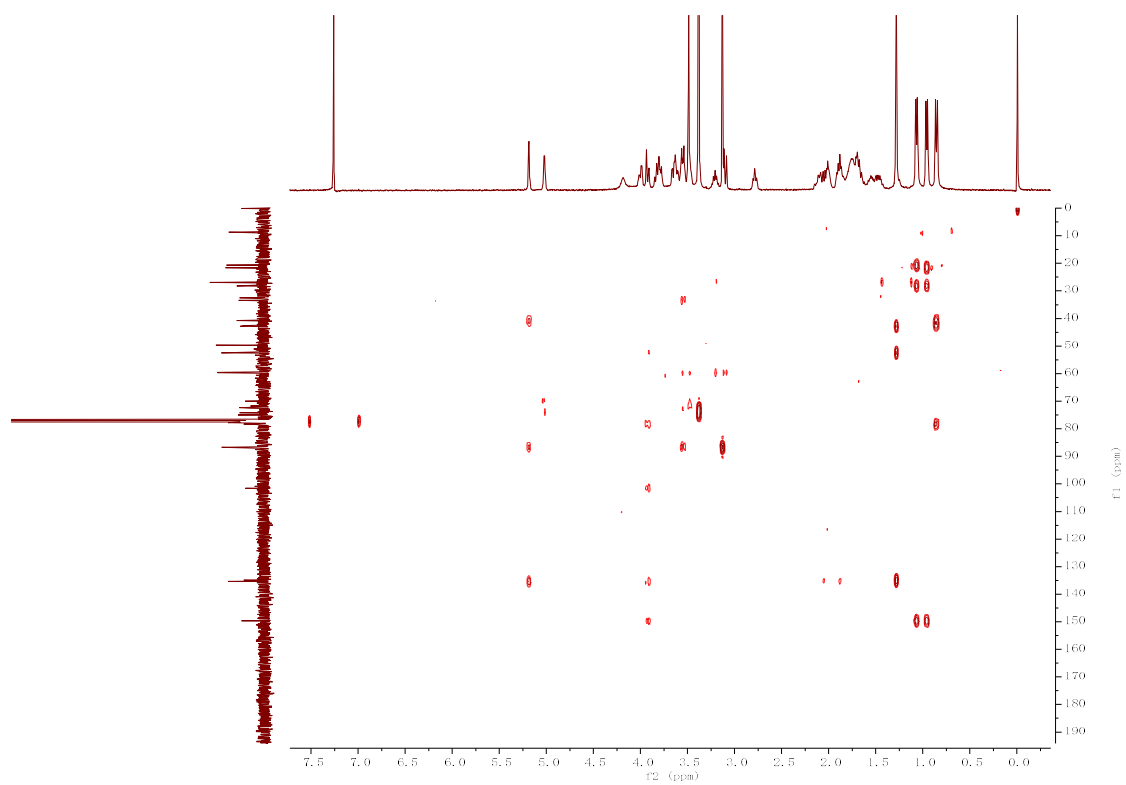


Figure S18. ^1H - ^1H COSY spectrum of dongtingnoid B (**2**) in CDCl_3

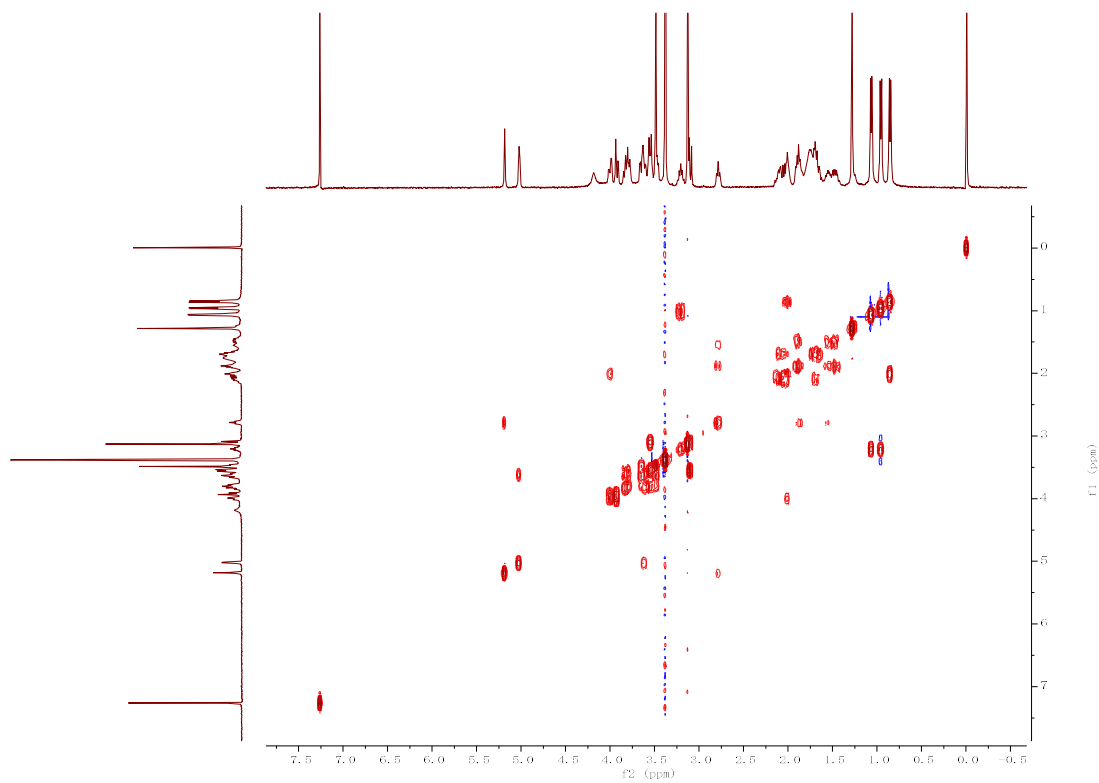


Figure S19. NOESY spectrum of dongtingnoid B (**2**) in CDCl_3

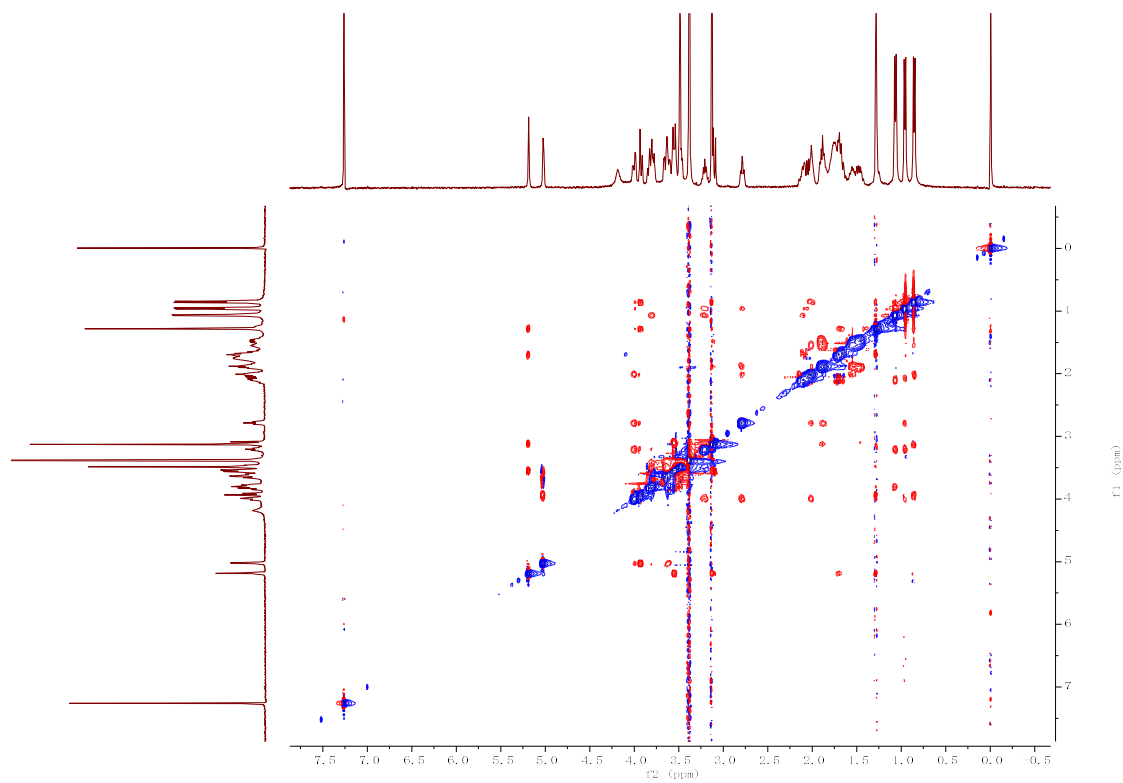


Figure S20. IR spectrum of dongtingnoid B (2)

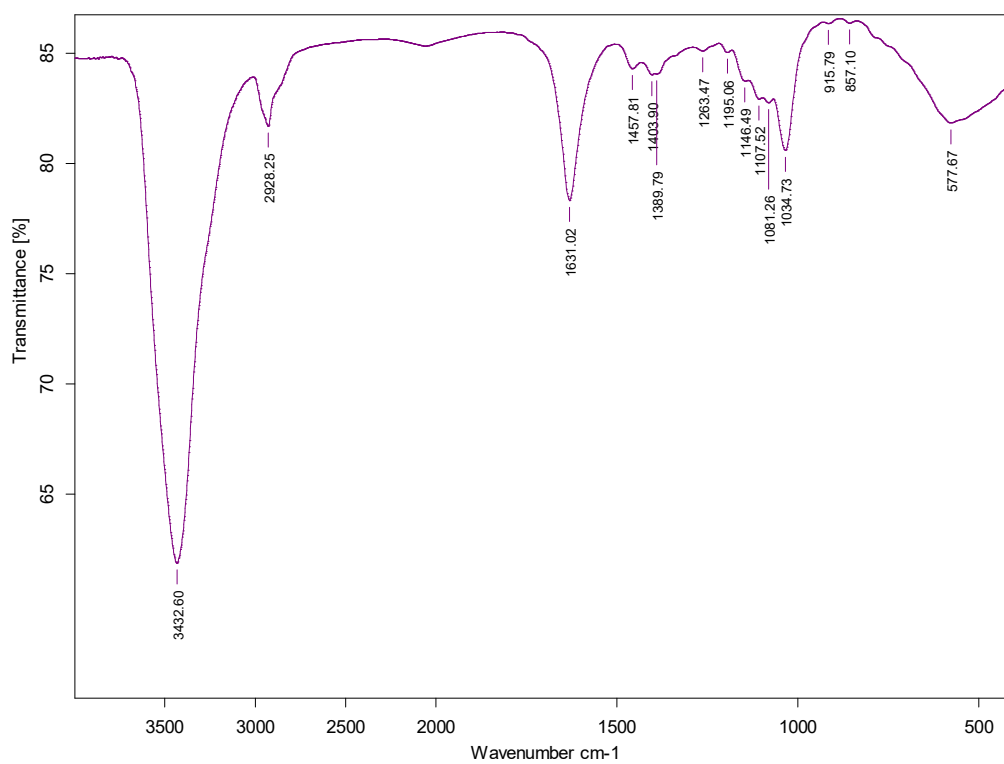


Figure S21. UV spectrum of dongtingnoid B (2)

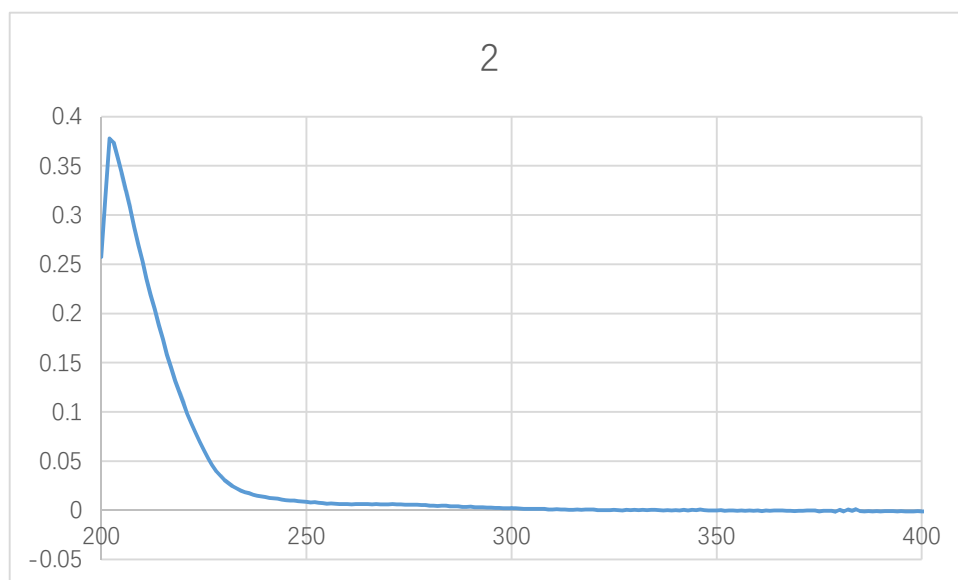


Figure S22. HRESIMS spectrum of dongtingnoid C (3)

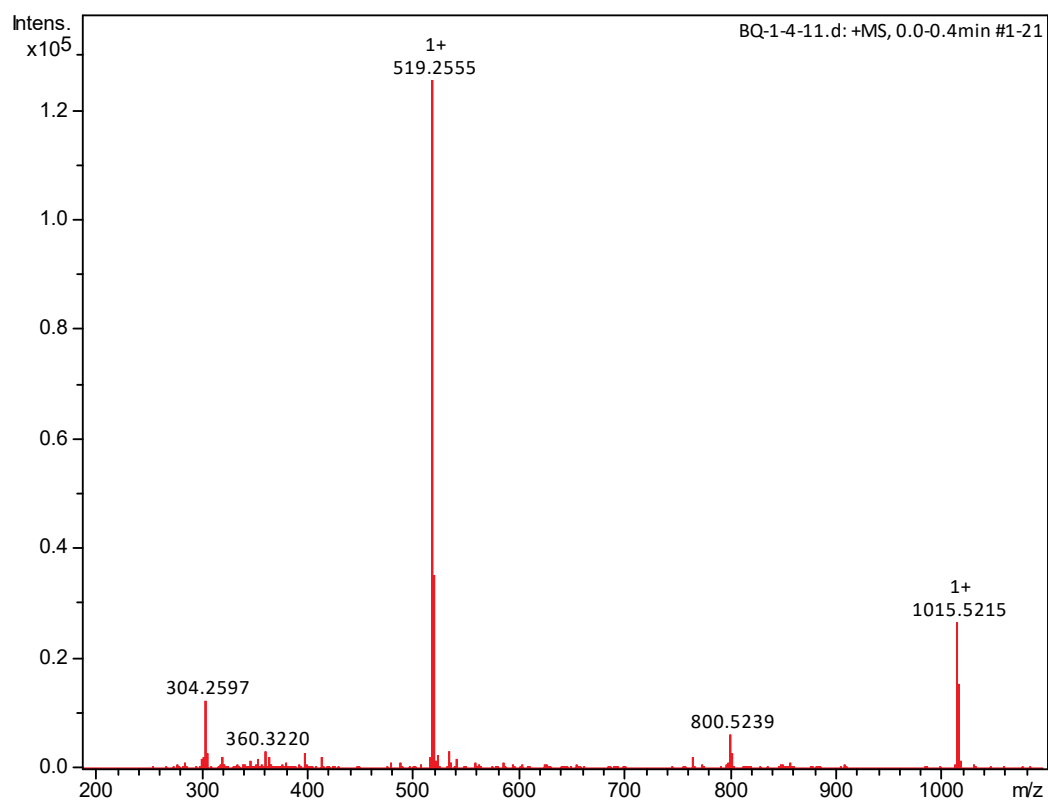


Figure S23. ¹H NMR spectrum of dongtingnoid C (3) in CDCl₃

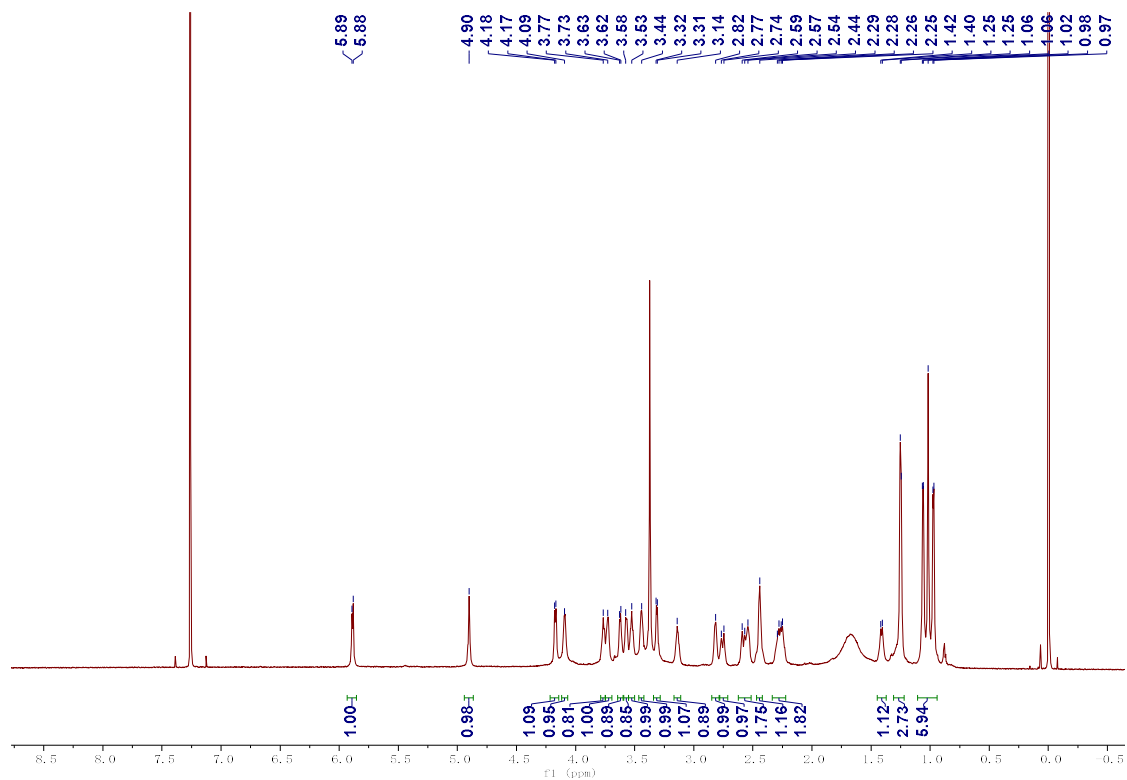


Figure S24. ^{13}C NMR spectrum of dongtingnoid C (**3**) in CDCl_3

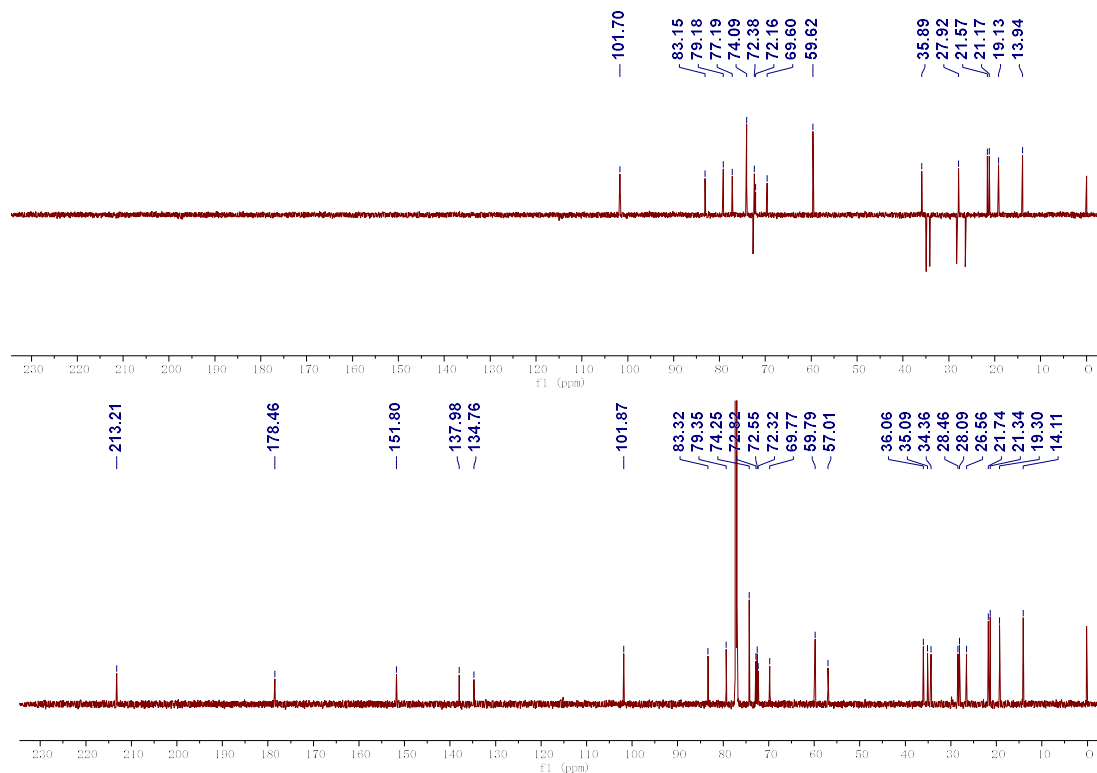


Figure S25. HSQC spectrum of dongtingnoid C (**3**) in CDCl_3

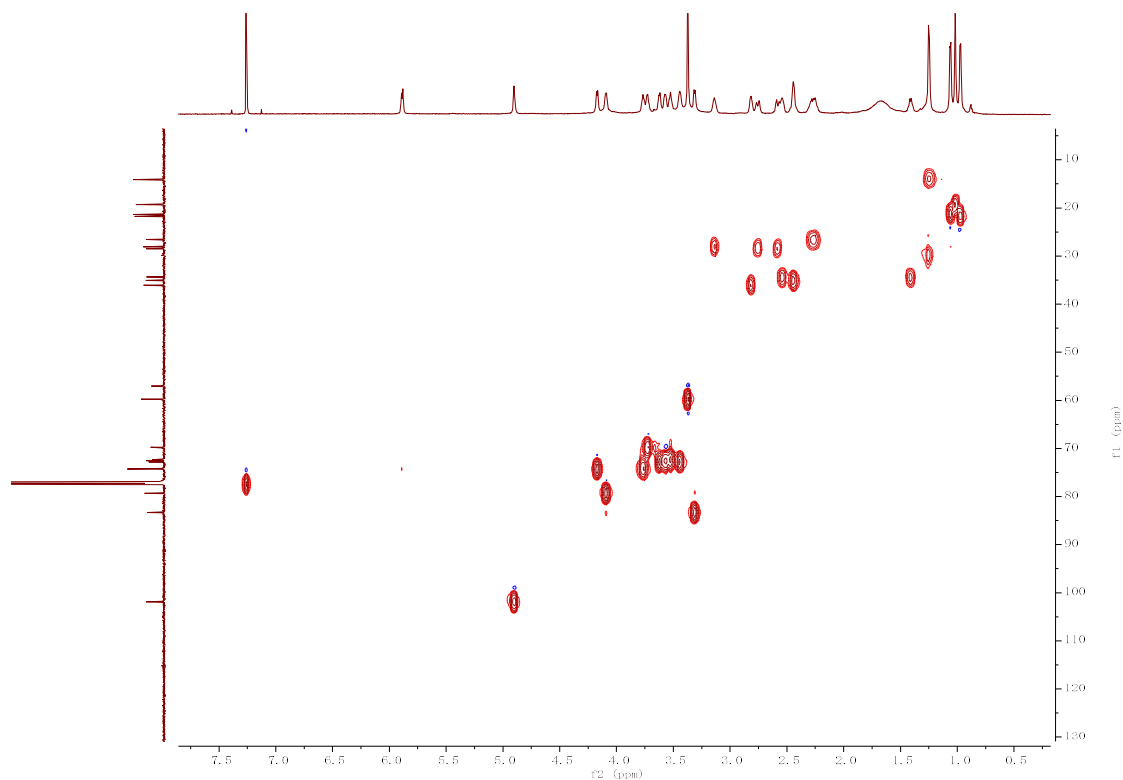


Figure S26. HMBC spectrum of dongtingnoid C (**3**) in CDCl₃

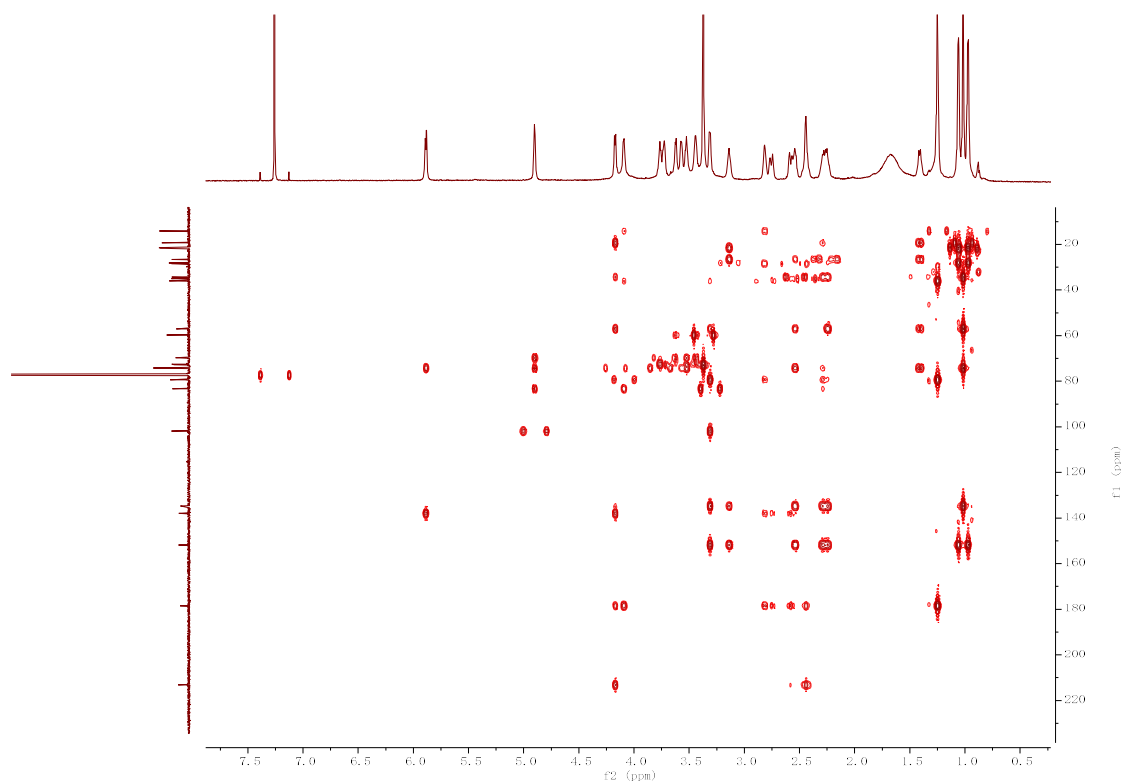


Figure S27. ¹H-¹H COSY spectrum of dongtingnoid C (**3**) in CDCl₃

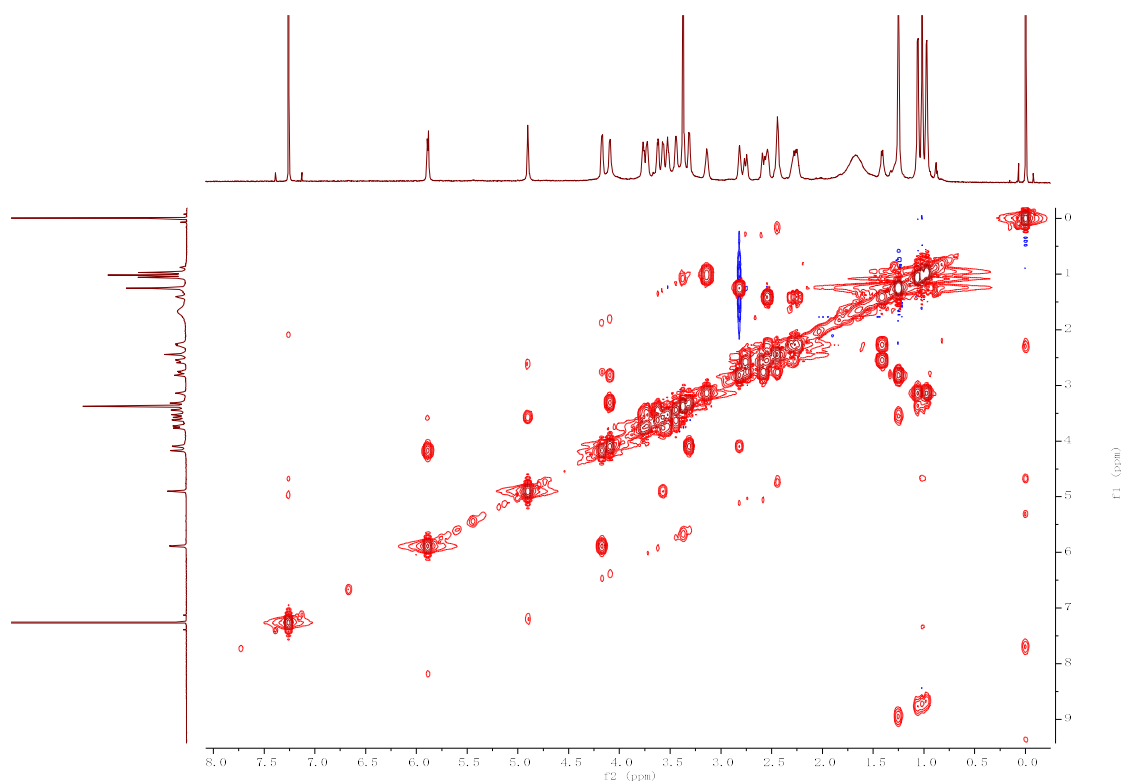


Figure S28. NOESY spectrum of dongtingnoid C (**3**) in CDCl₃

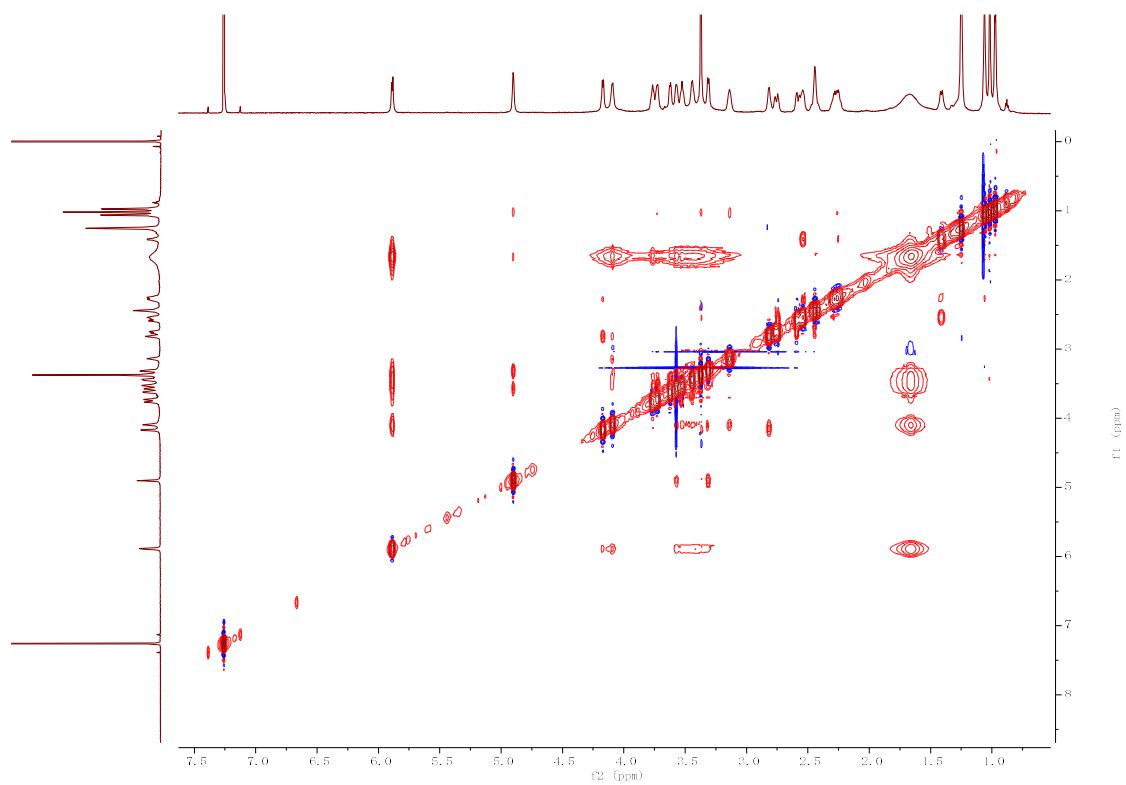


Figure S29. IR spectrum of dongtingnoid C (**3**)

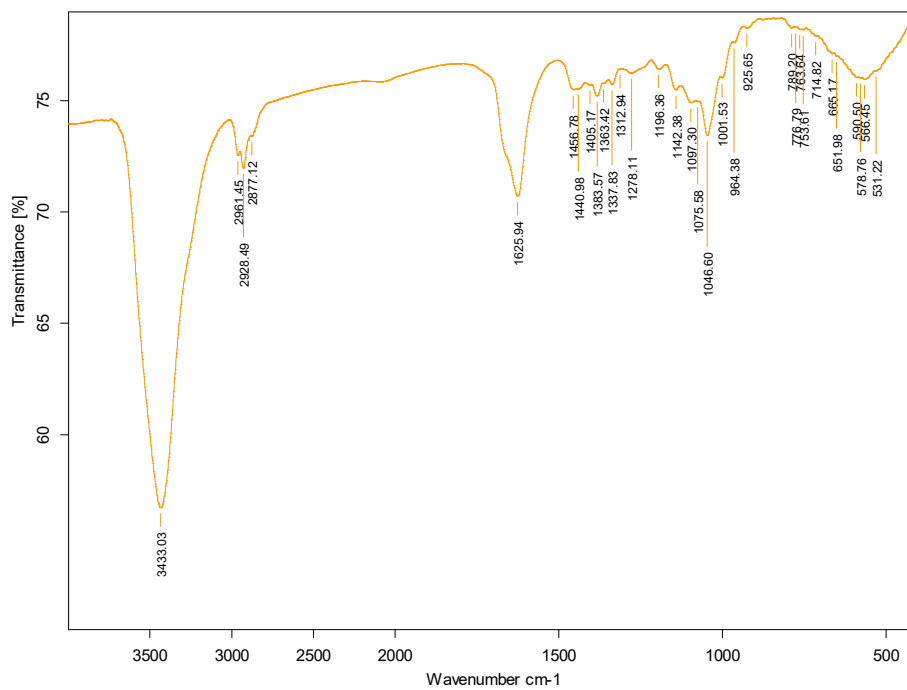


Figure S30. UV spectrum of dongtingnoid C (3)

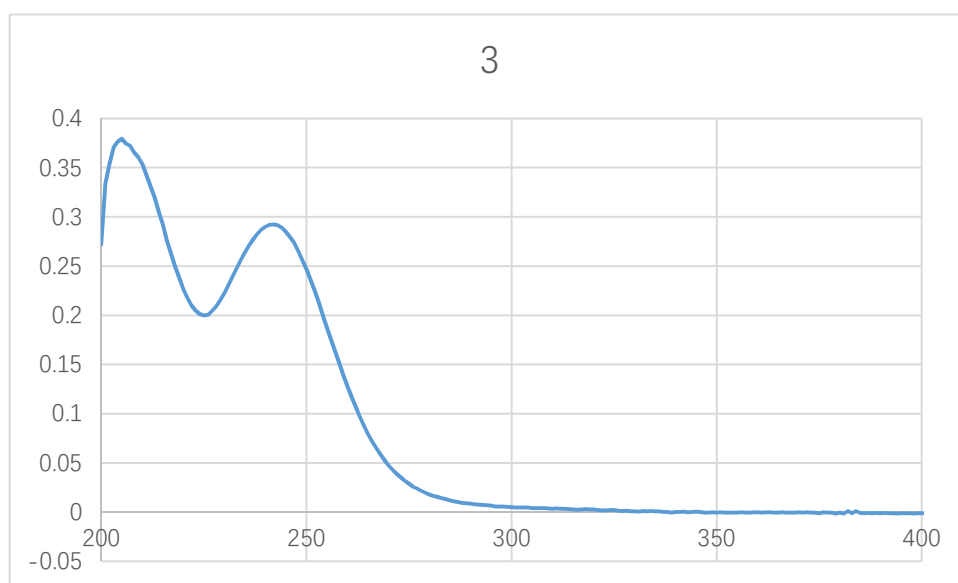


Figure S31. HRESIMS spectrum of dongtingnoid D (4)

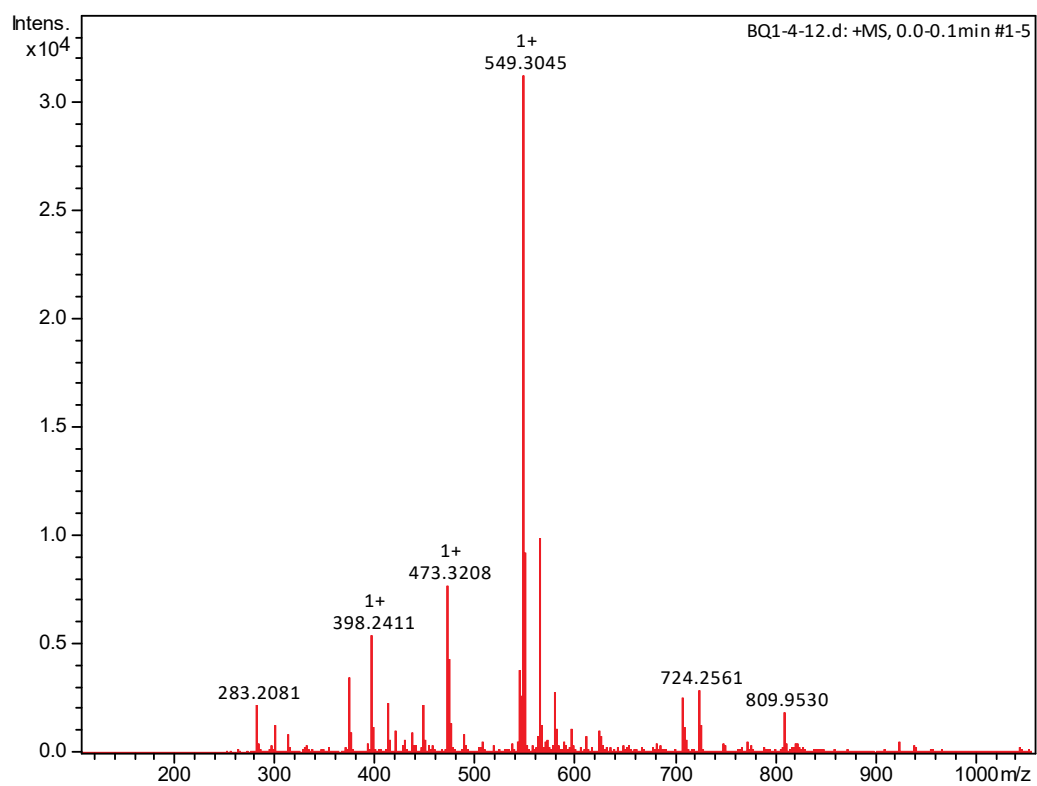


Figure S32. ^1H NMR spectrum of dongtingnoid D (**4**) in CDCl_3

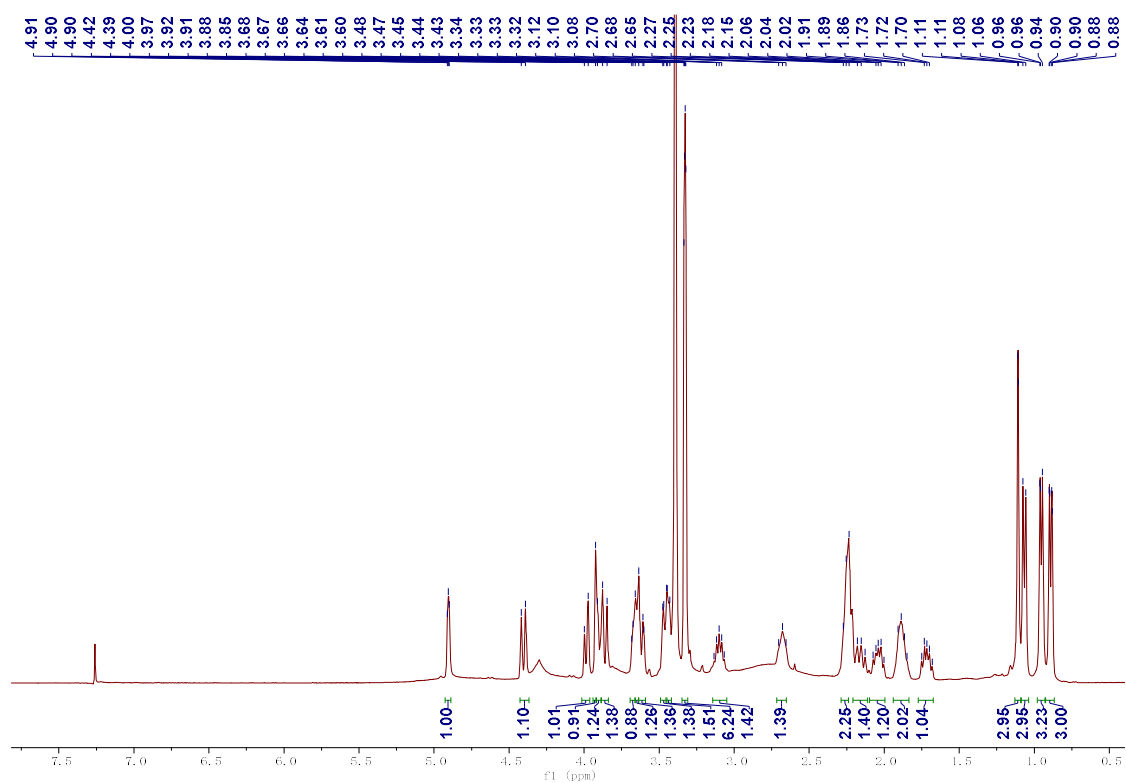


Figure S33. ^{13}C NMR spectrum of dongtingnoid D (**4**) in CDCl_3

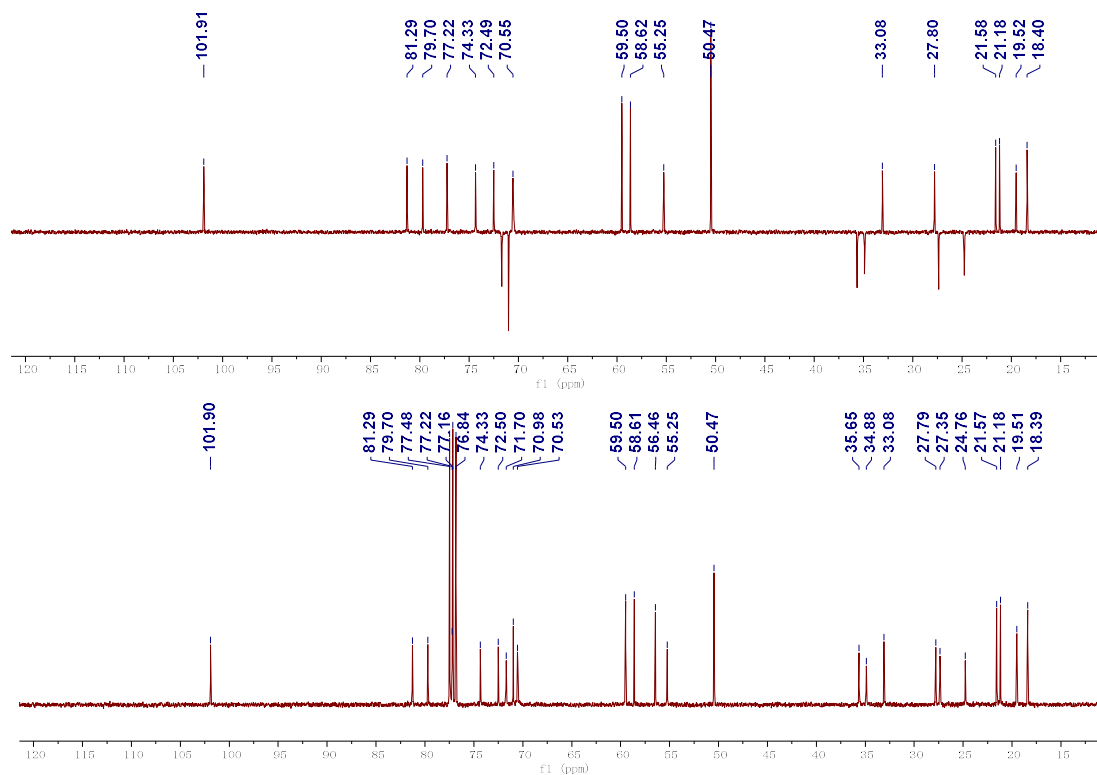


Figure S34. HSQC spectrum of dongtingnoid D (**4**) in CDCl₃

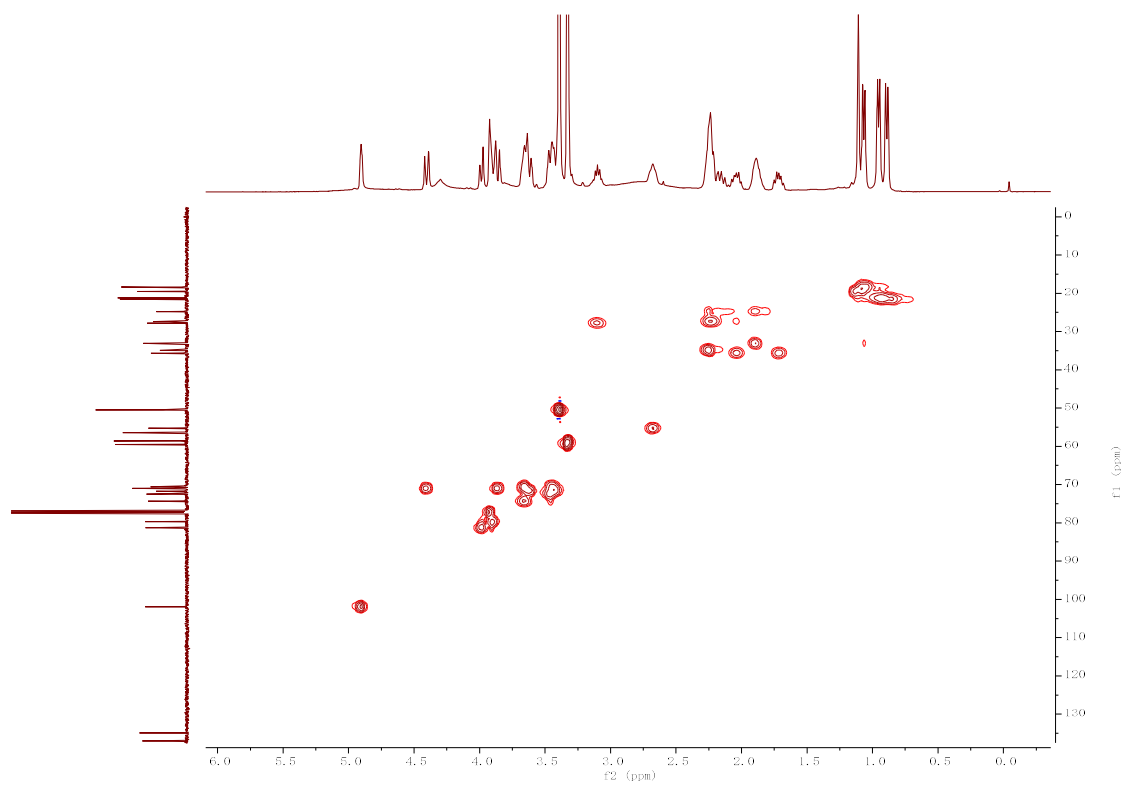


Figure S35. HMBC spectrum of dongtingnoid D (**4**) in CDCl₃

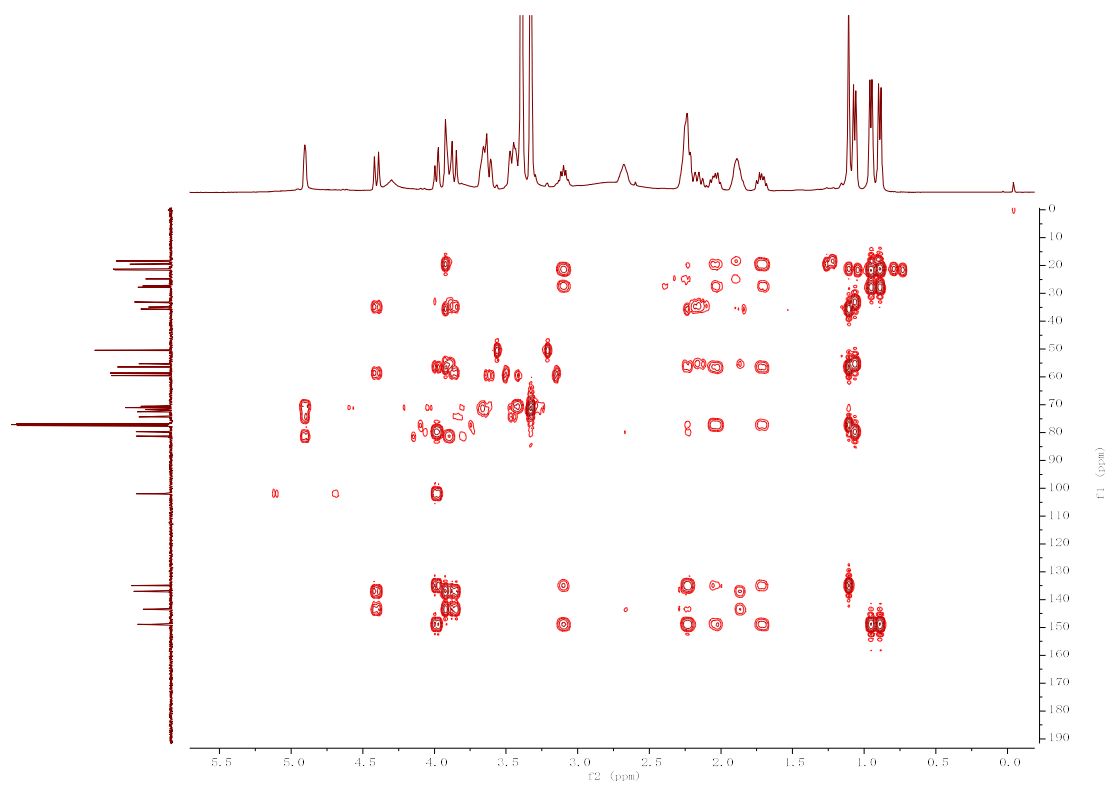


Figure S36. ^1H - ^1H COSY spectrum of dongtingnoid D (**4**) in CDCl_3

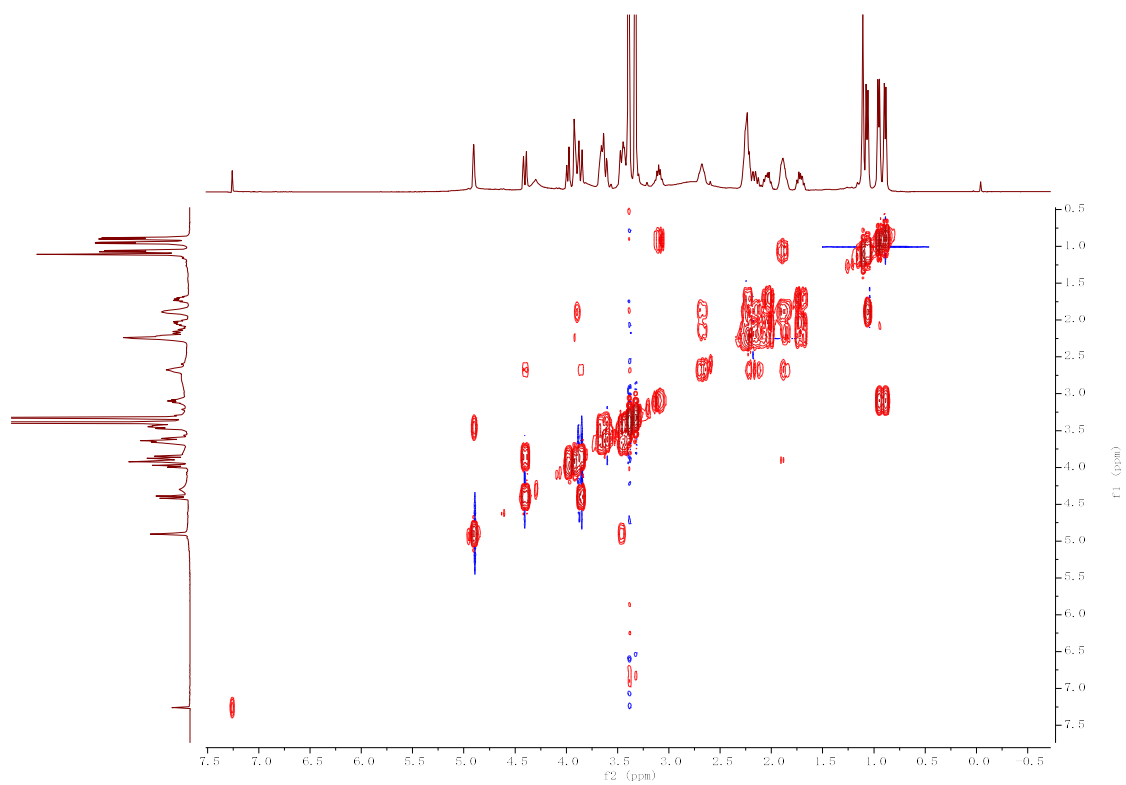


Figure S37. NOESY spectrum of dongtingnoid D (**4**) in CDCl_3

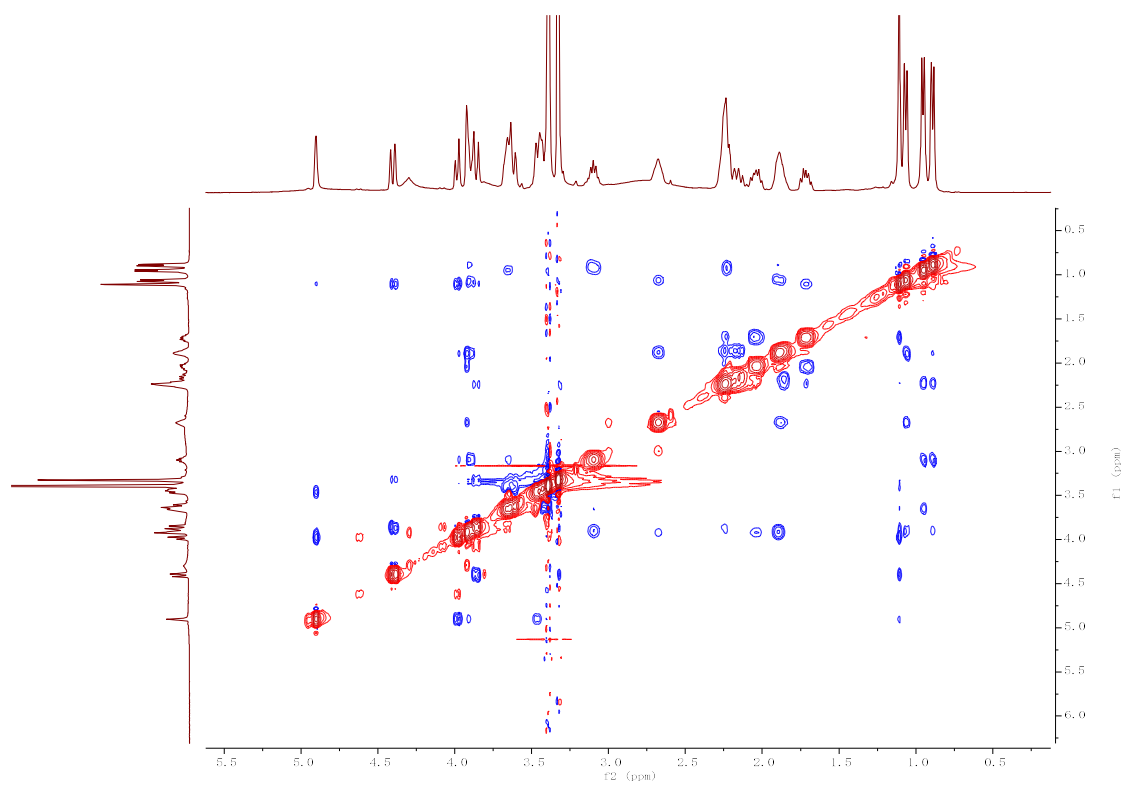


Figure S38. IR spectrum of dongtingnoid D (4)

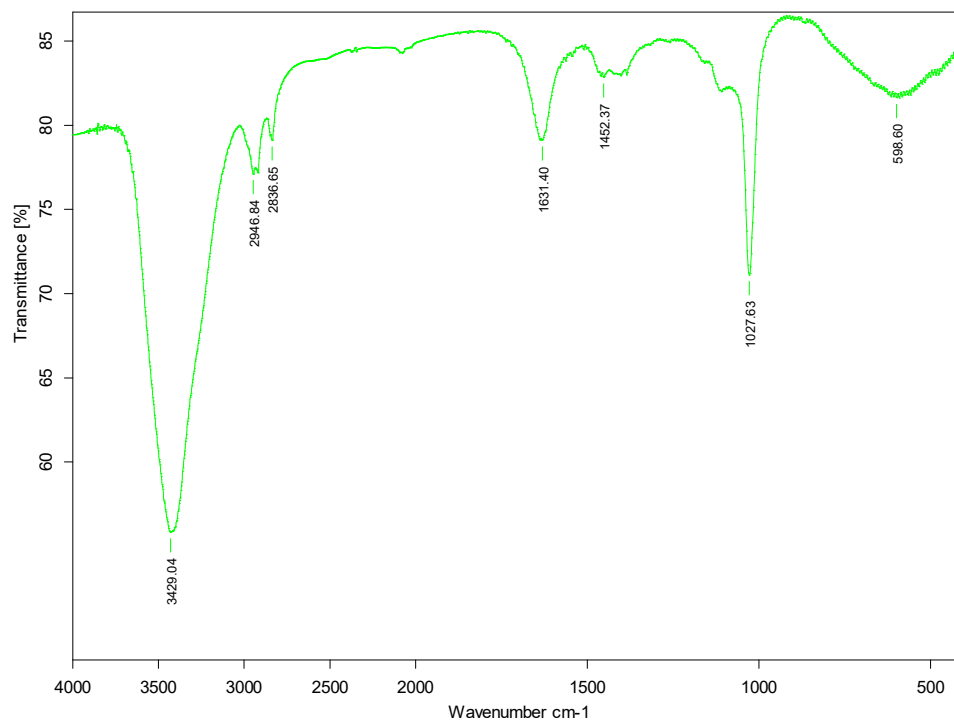


Figure S39. UV spectrum of dongtingnoid D (4)

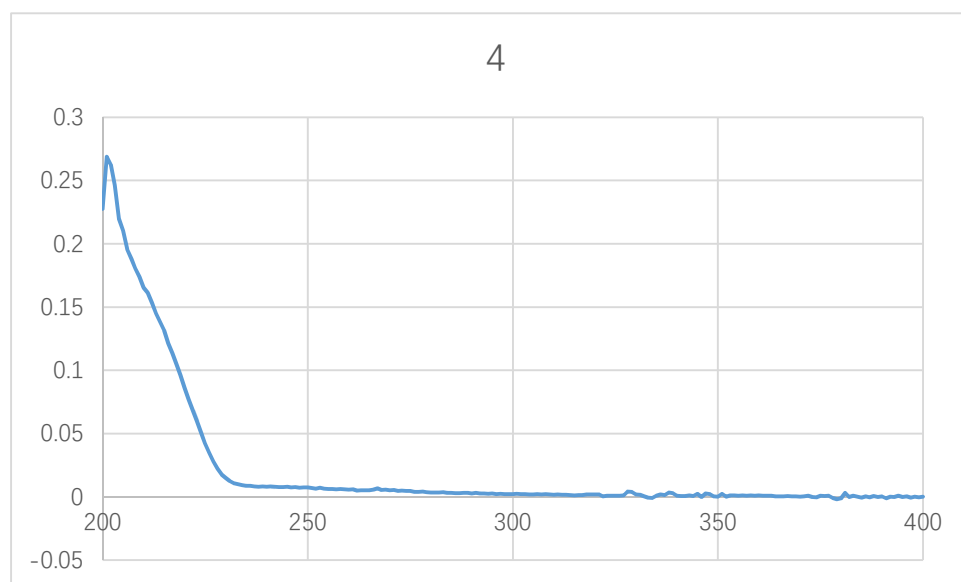


Figure S40. HRESIMS spectrum of dongtingnoid E (5)

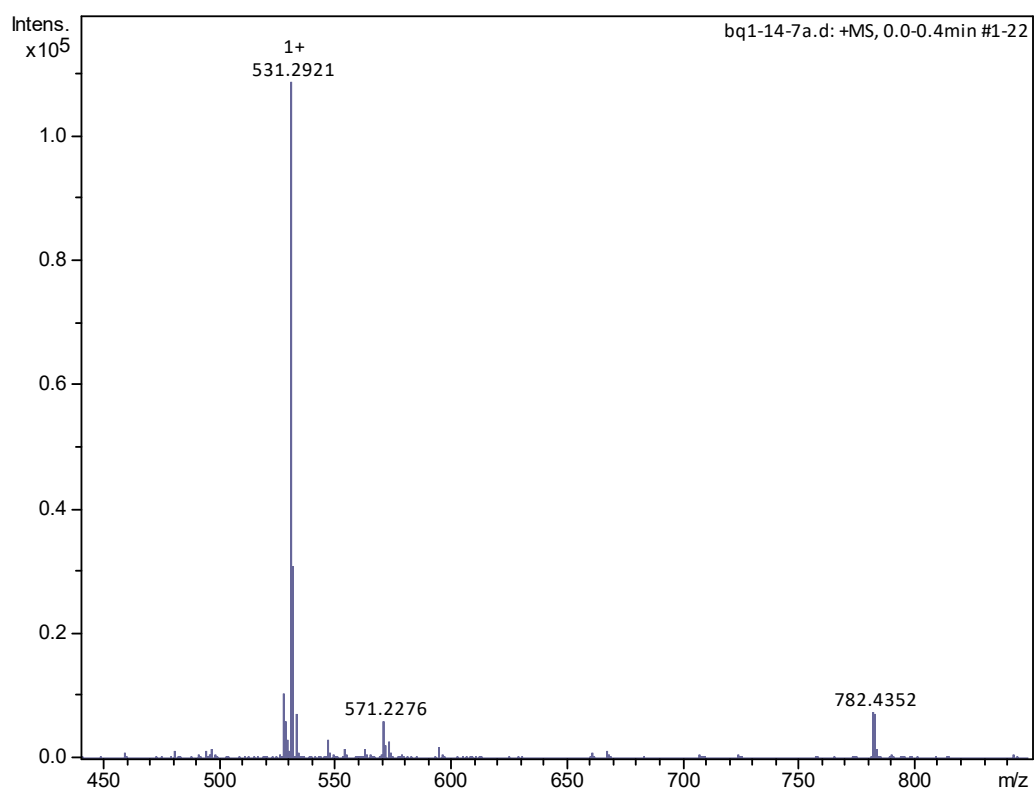


Figure S41. ¹H NMR spectrum of dongtingnoid E (5) in CDCl₃

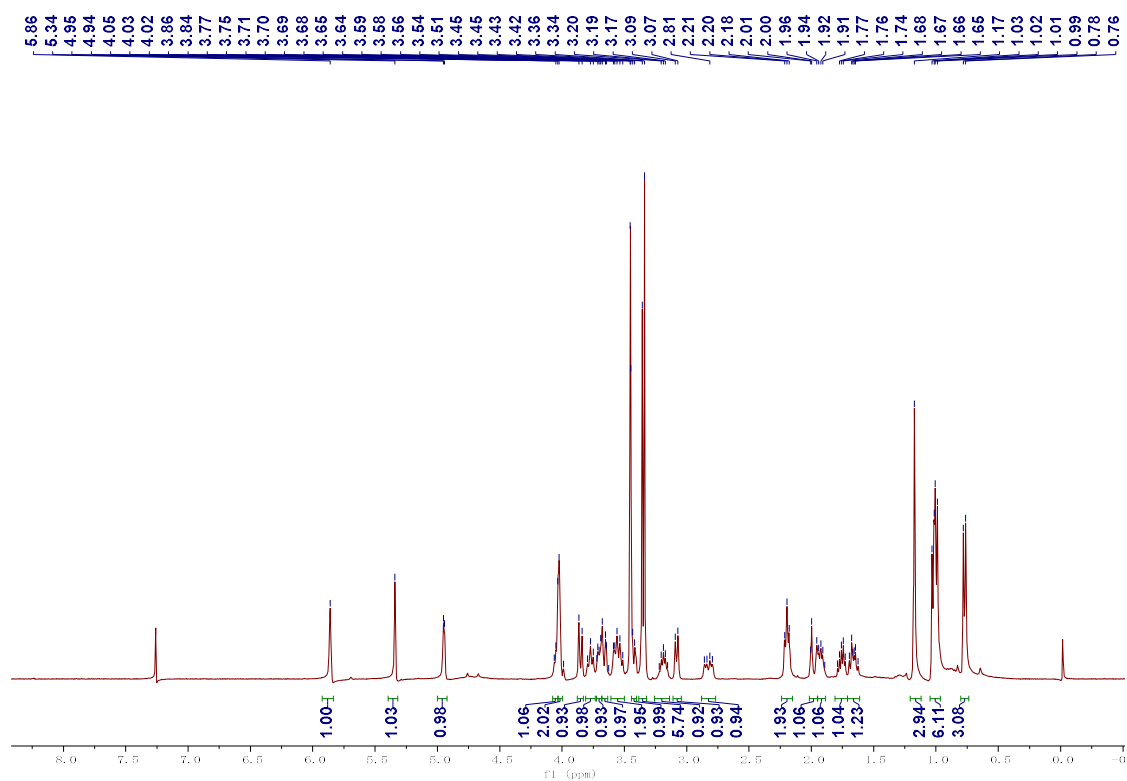


Figure S42. ^{13}C NMR spectrum of dongtingnoid E (**5**) in CDCl_3

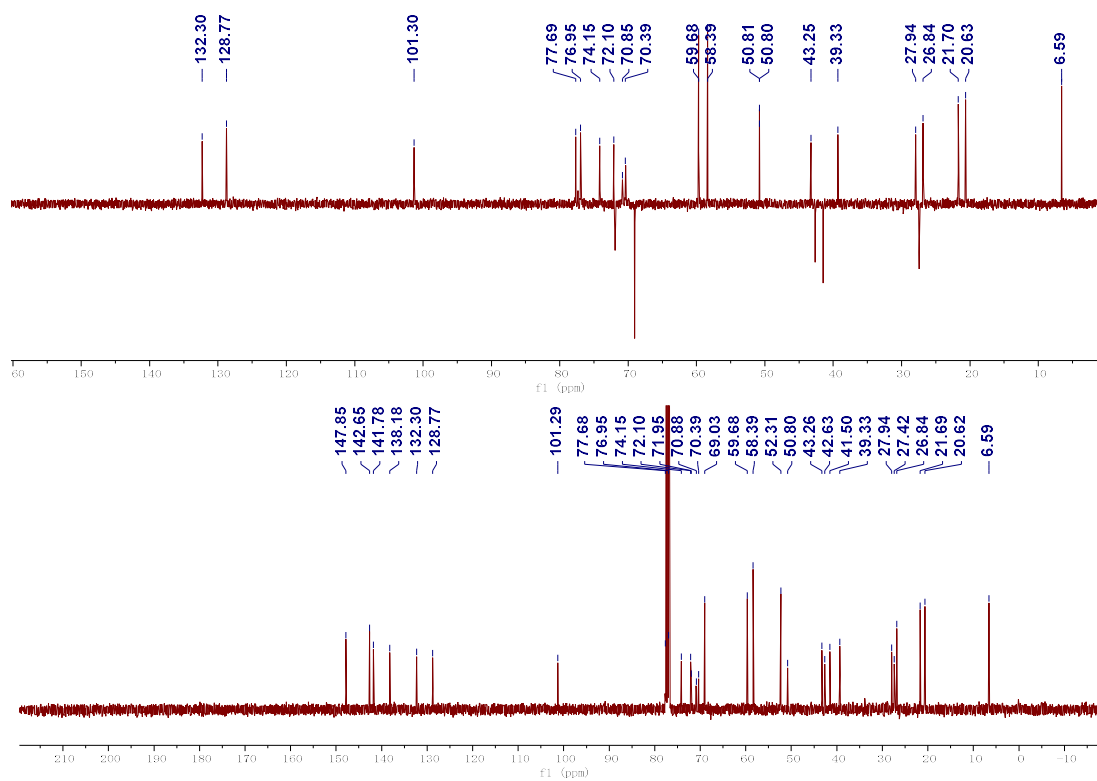


Figure S43. HSQC spectrum of dongtingnoid E (**5**) in CDCl_3

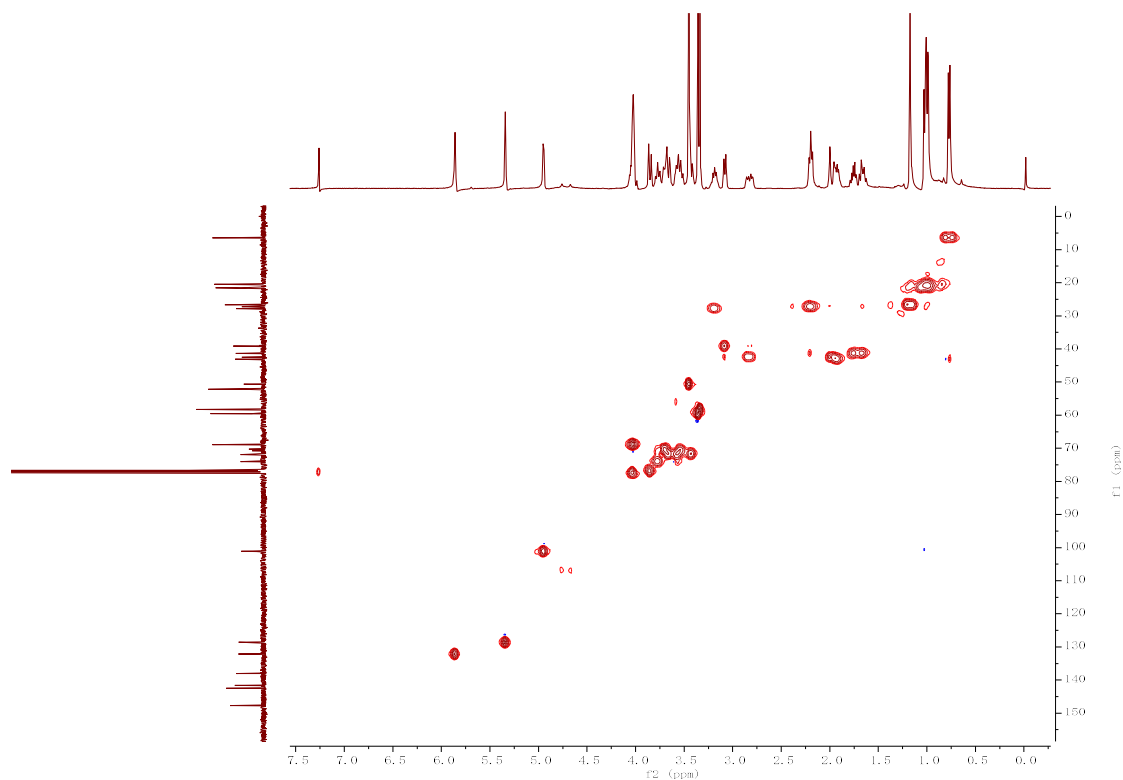


Figure S44. HMBC spectrum of dongtingnoid E (**5**) in CDCl₃

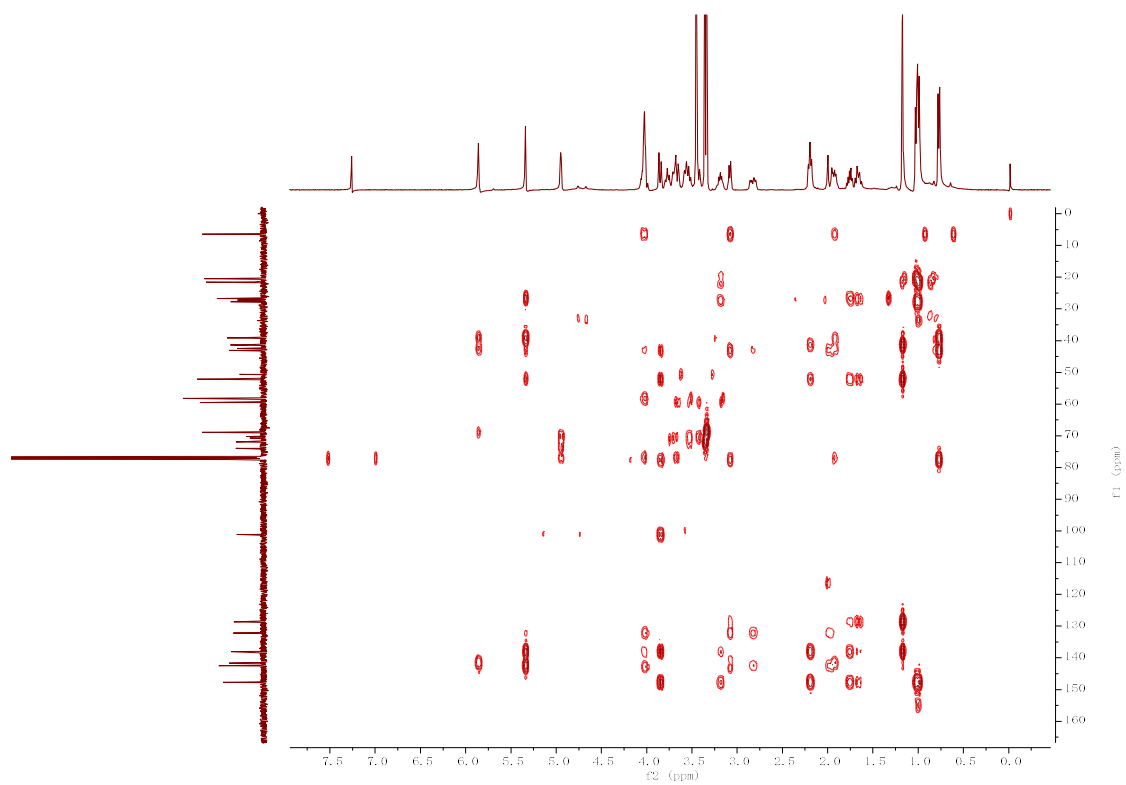


Figure S45. ¹H-¹H COSY spectrum of dongtingnoid E (**5**) in CDCl₃

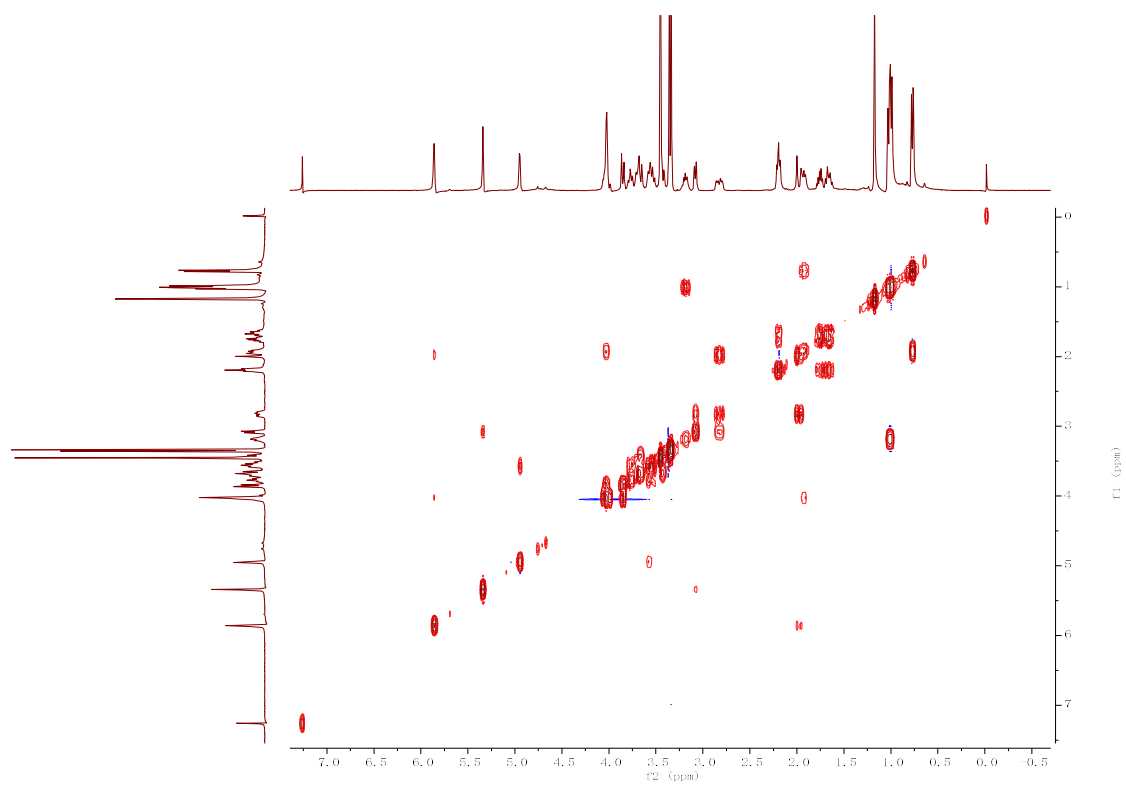


Figure S46. NOESY spectrum of dongtingnoid E (5) in CDCl₃

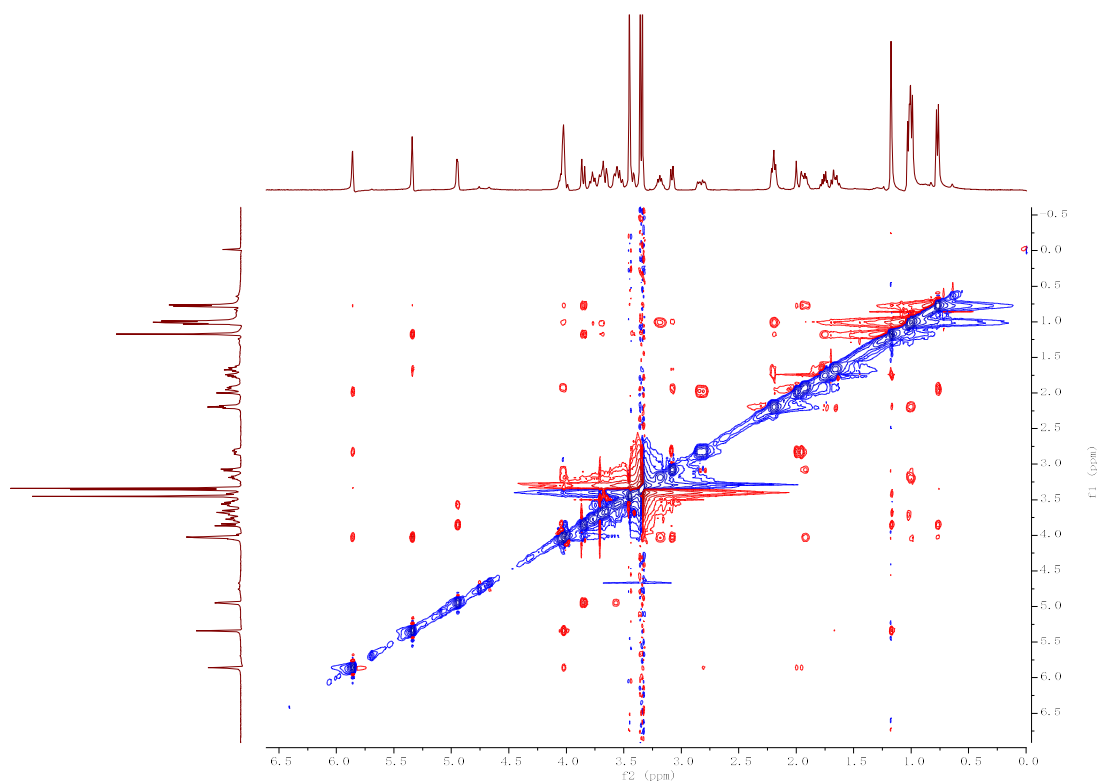


Figure S47. IR spectrum of dongtingnoid E (5)

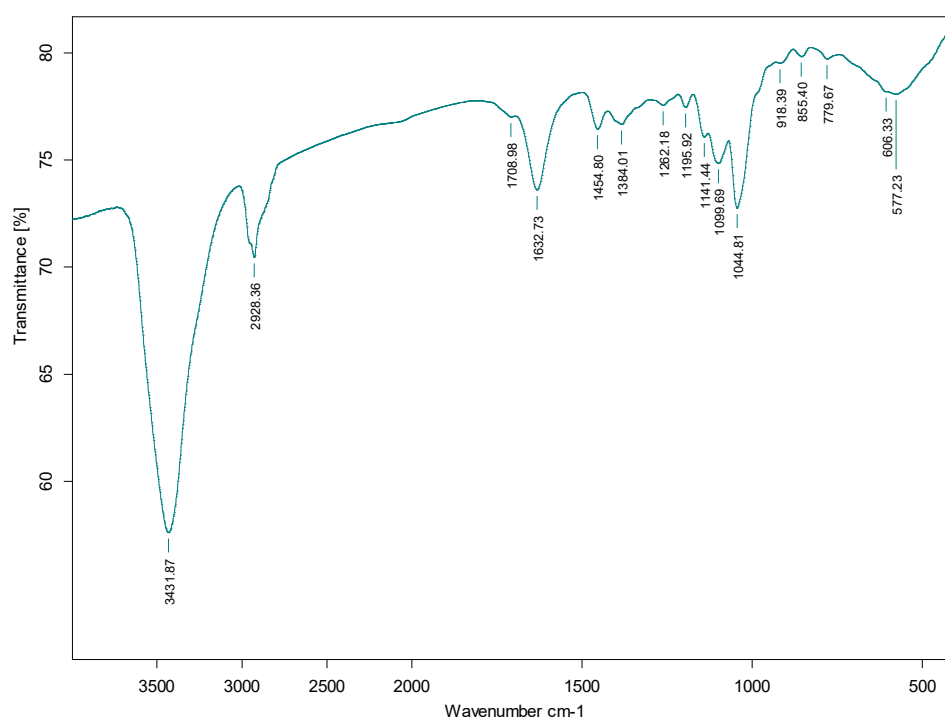


Figure S48. UV spectrum of dongtingnoid E (5)

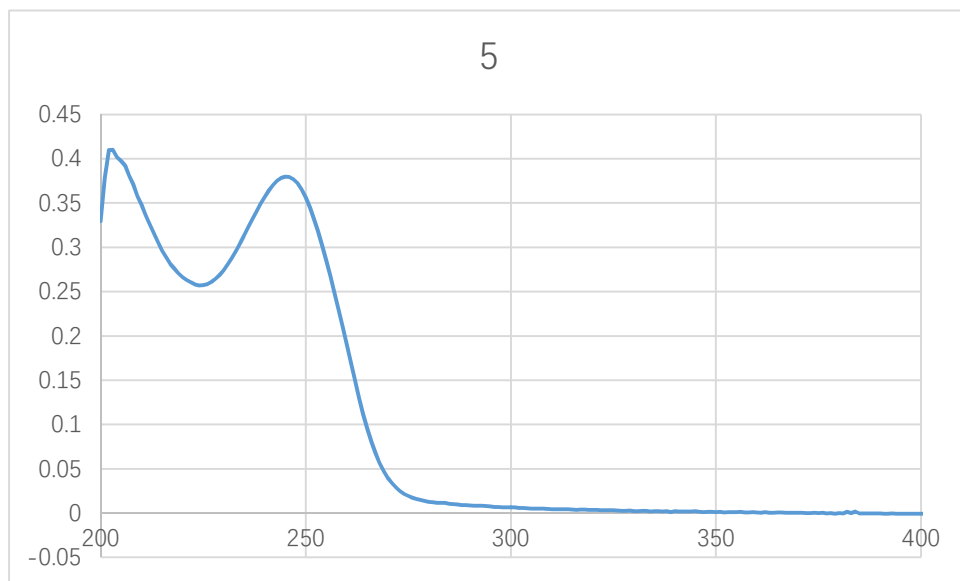


Figure S49. HRESIMS spectrum of dongtingnoid F (6)

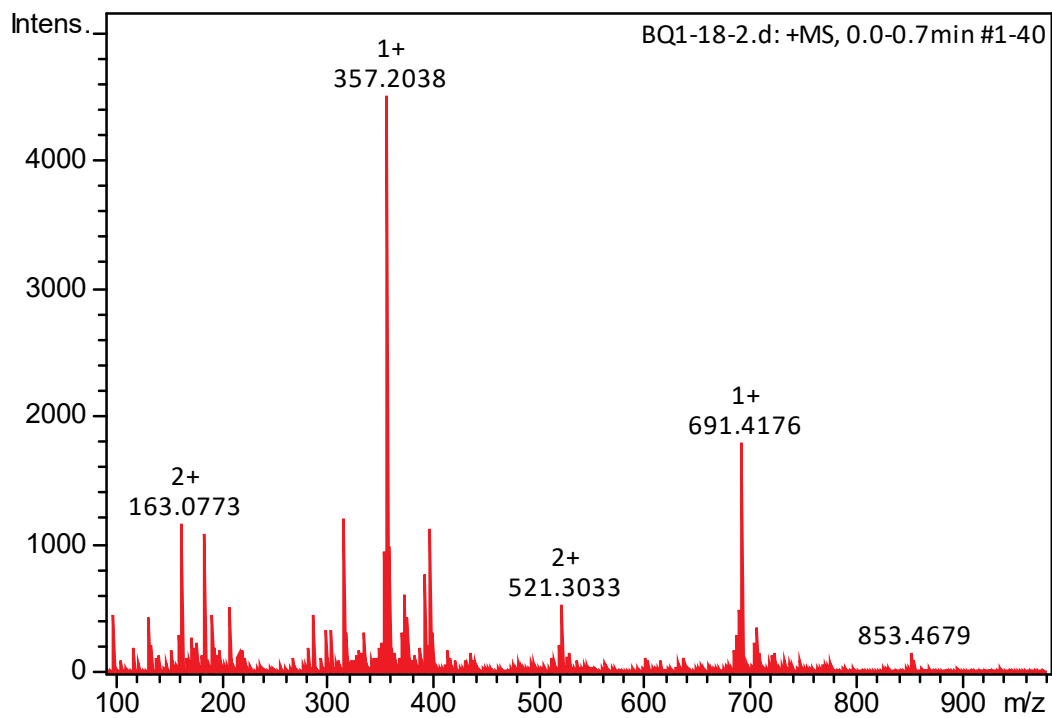


Figure S50. ¹H NMR spectrum of dongtingnoid F (6) in CDCl₃

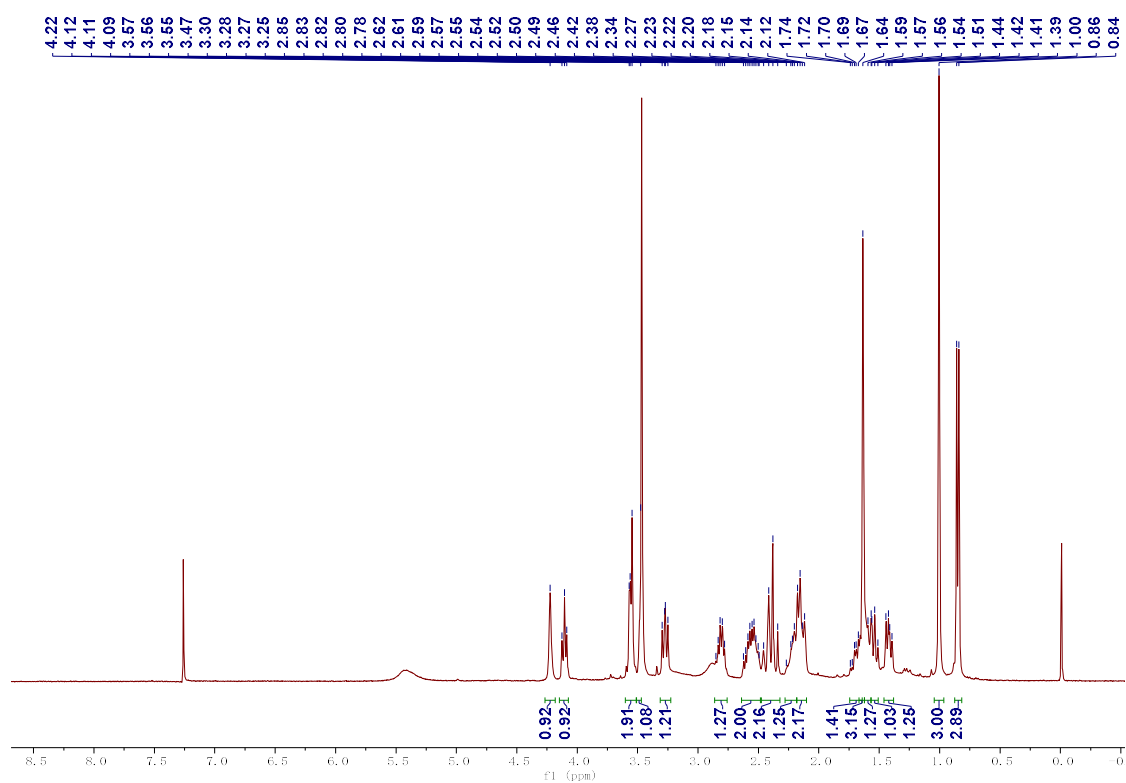


Figure S51. ¹³C NMR spectrum of dongtingnoid F (6) in CDCl₃

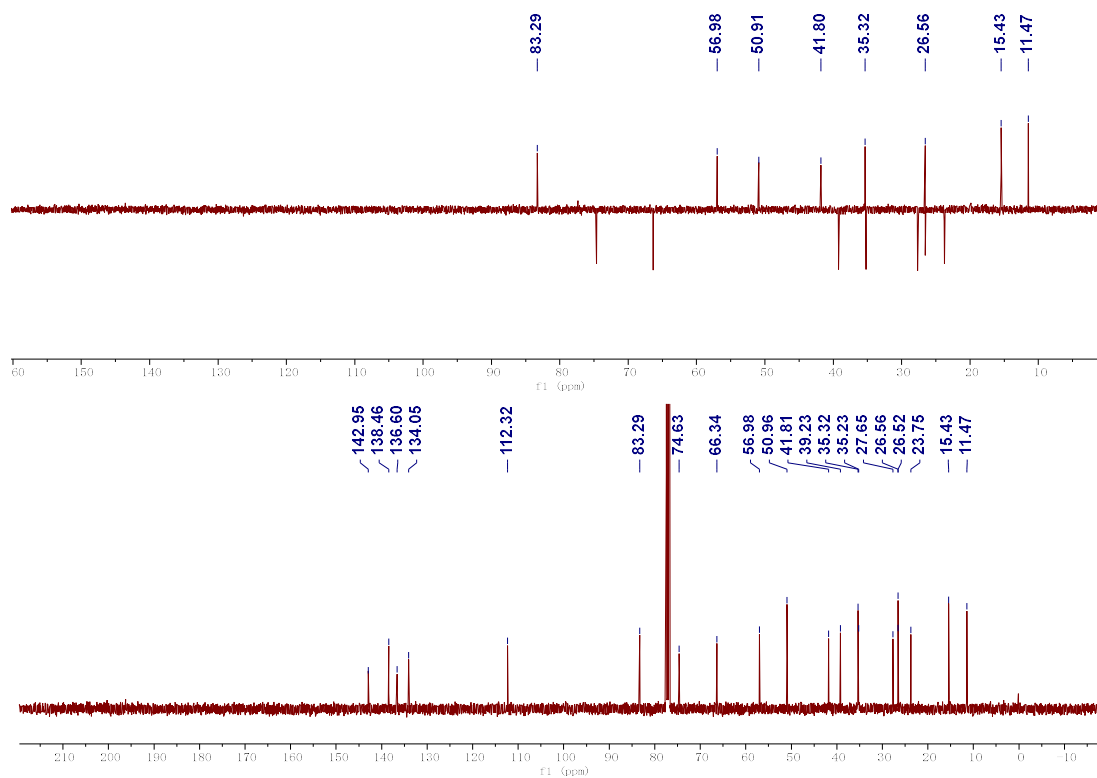


Figure S52. HSQC spectrum of dongtingnoid F (**6**) in CDCl₃

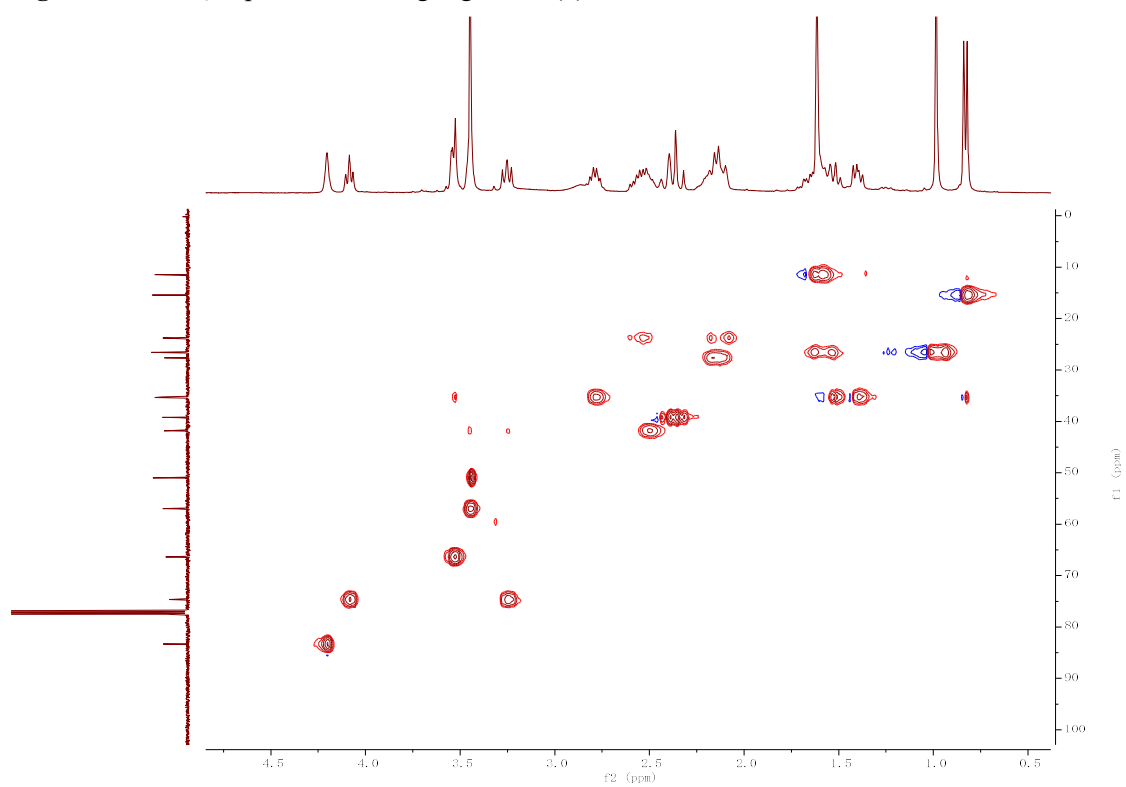


Figure S53. HMBC spectrum of dongtingnoid F (**6**) in CDCl₃

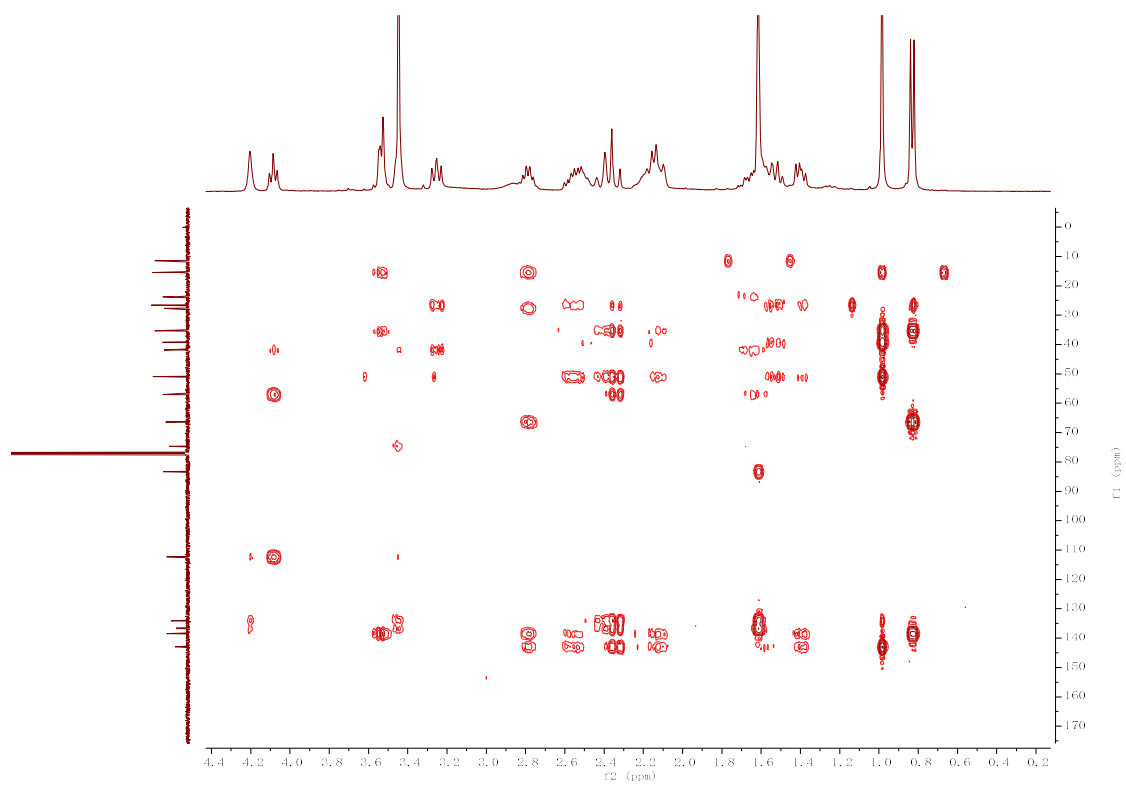


Figure S54. ^1H - ^1H COSY spectrum of dongtingnoid F (**6**) in CDCl_3

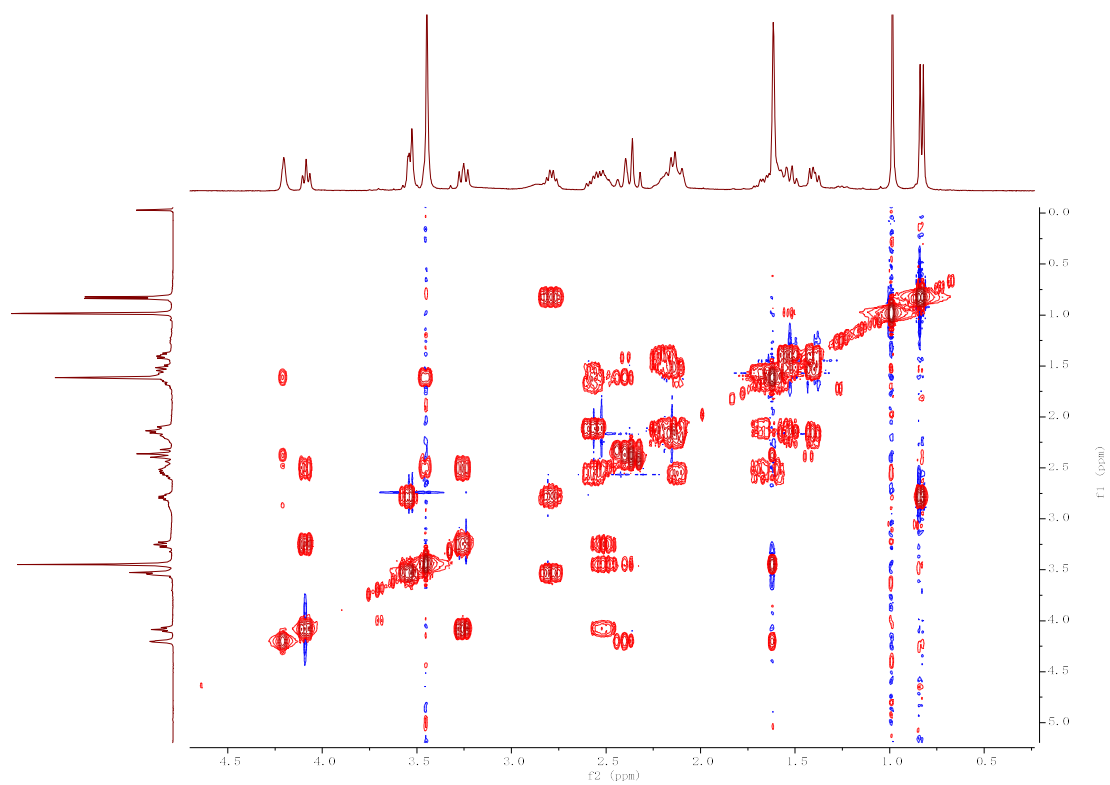


Figure S55. NOESY spectrum of dongtingnoid F (**6**) in CDCl_3

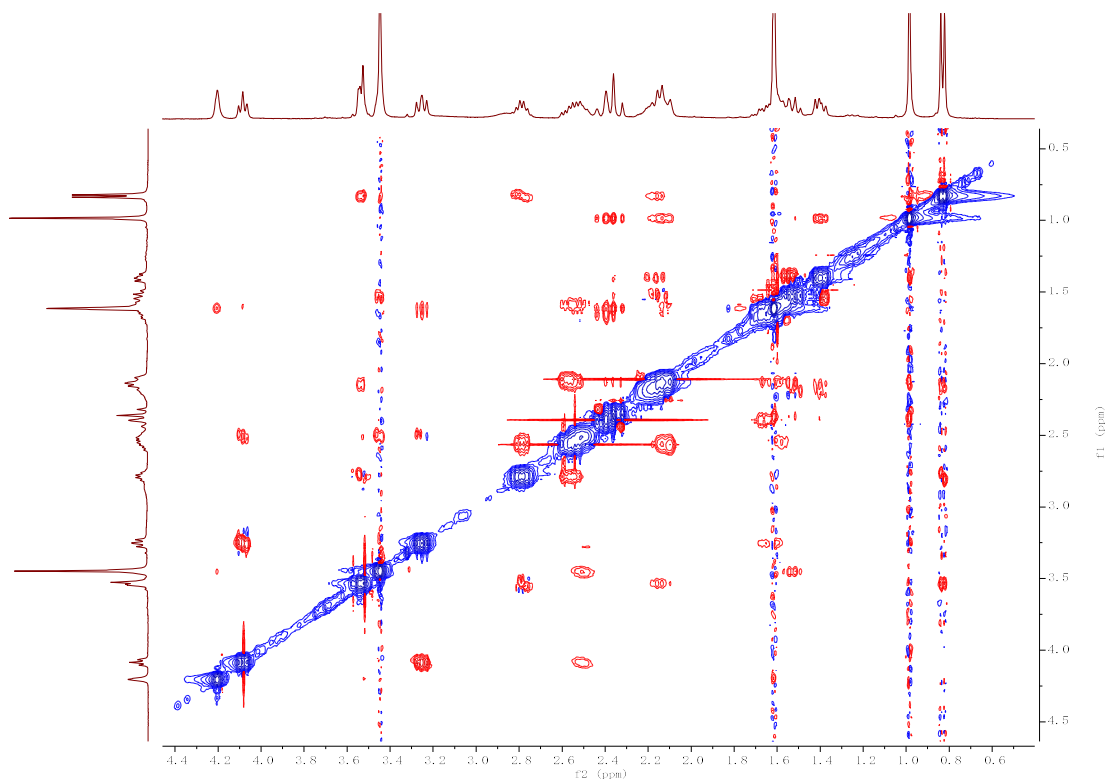


Figure S56. IR spectrum of dongtingnoid F (6)

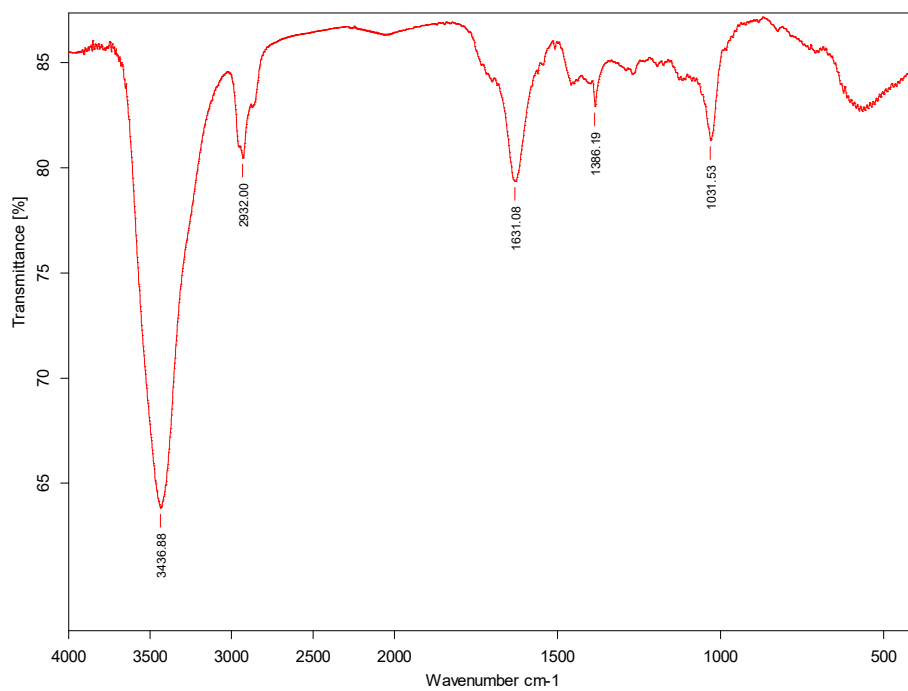


Figure S57. UV spectrum of dongtingnoid F (6)

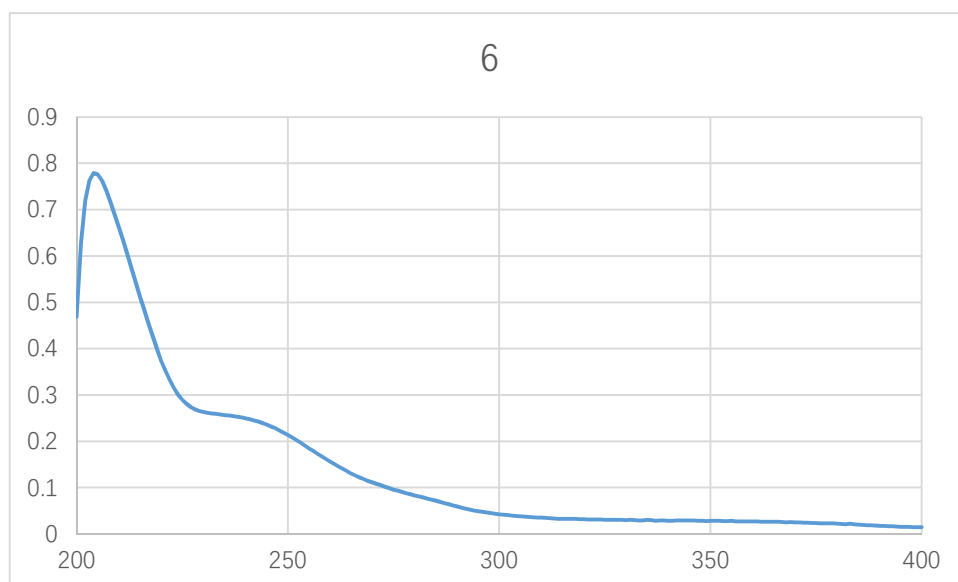


Figure S58. HRESIMS spectrum of dongtingnoid G (7)

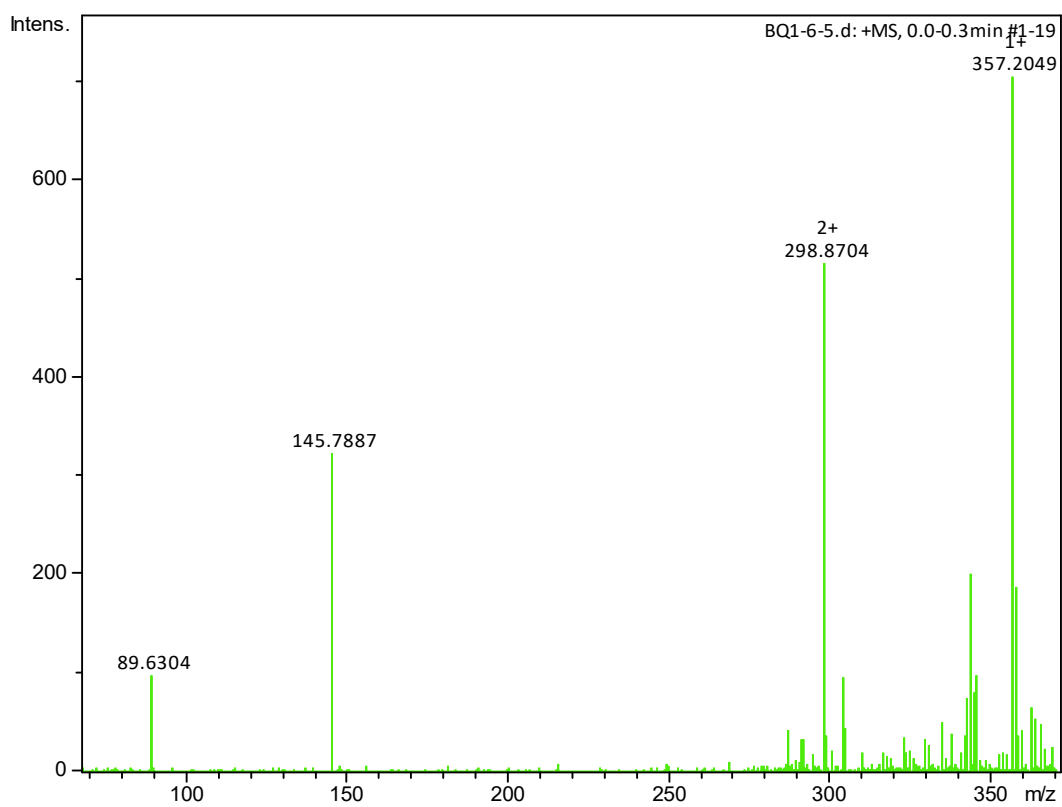


Figure S59. ^1H NMR spectrum of dongtingnoid G (7) in CDCl_3

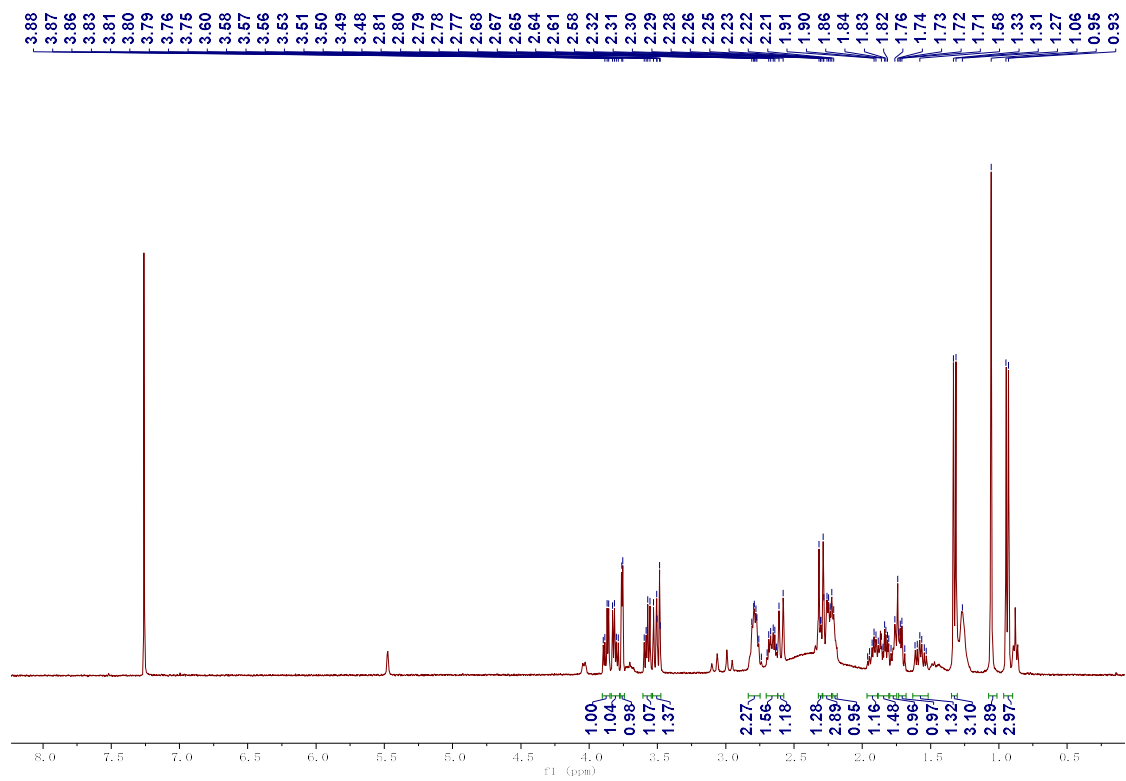


Figure S60. ^{13}C NMR spectrum of dongtingnoid G (7) in CDCl_3

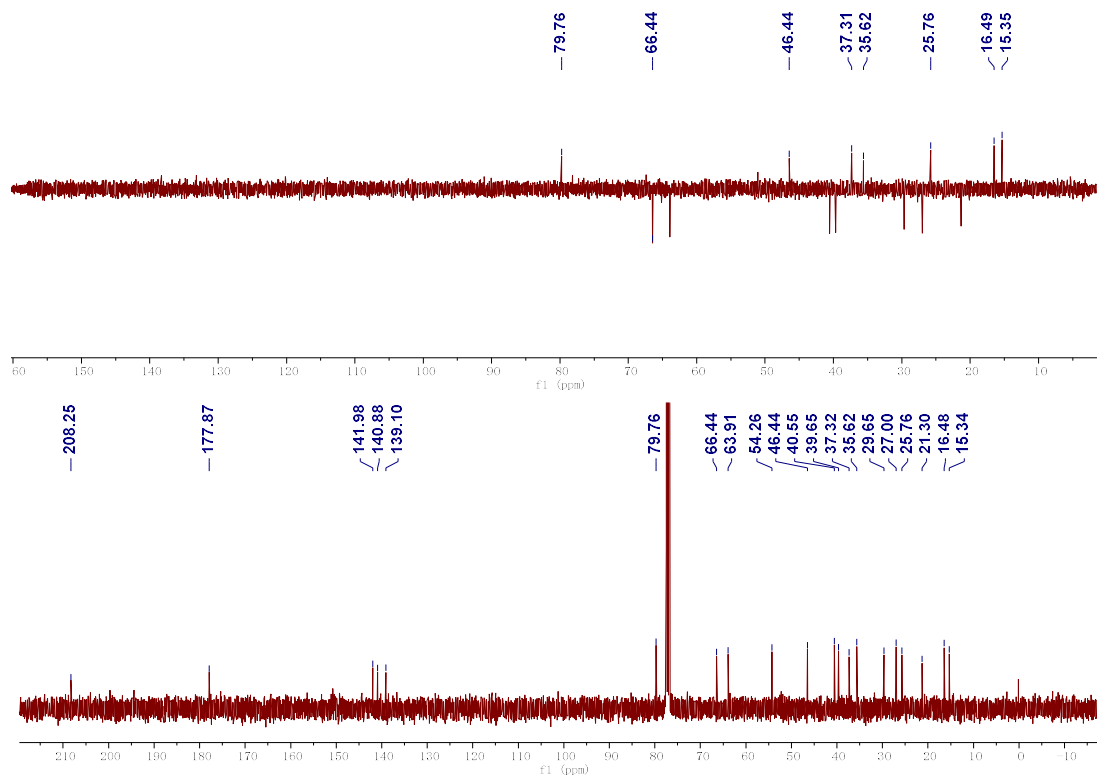


Figure S61. HSQC spectrum of dongtingnoid G (7) in CDCl_3

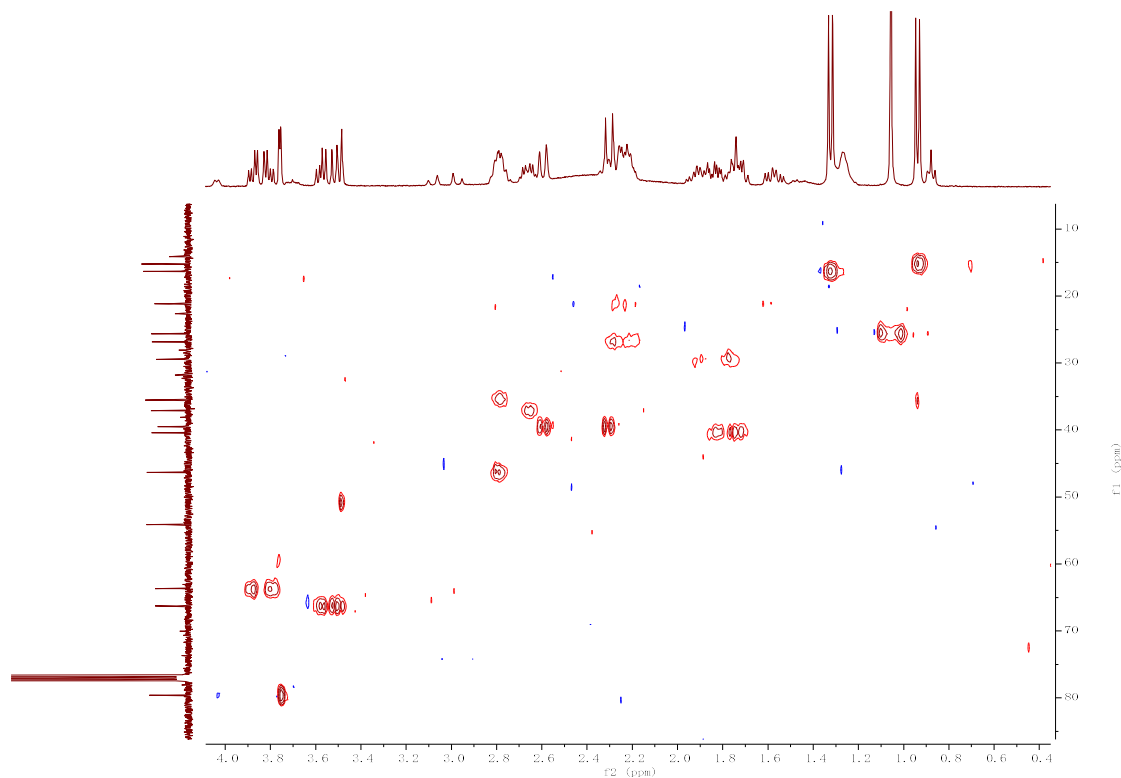


Figure S62. HMBC spectrum of dongtingnoid G (7) in CDCl₃

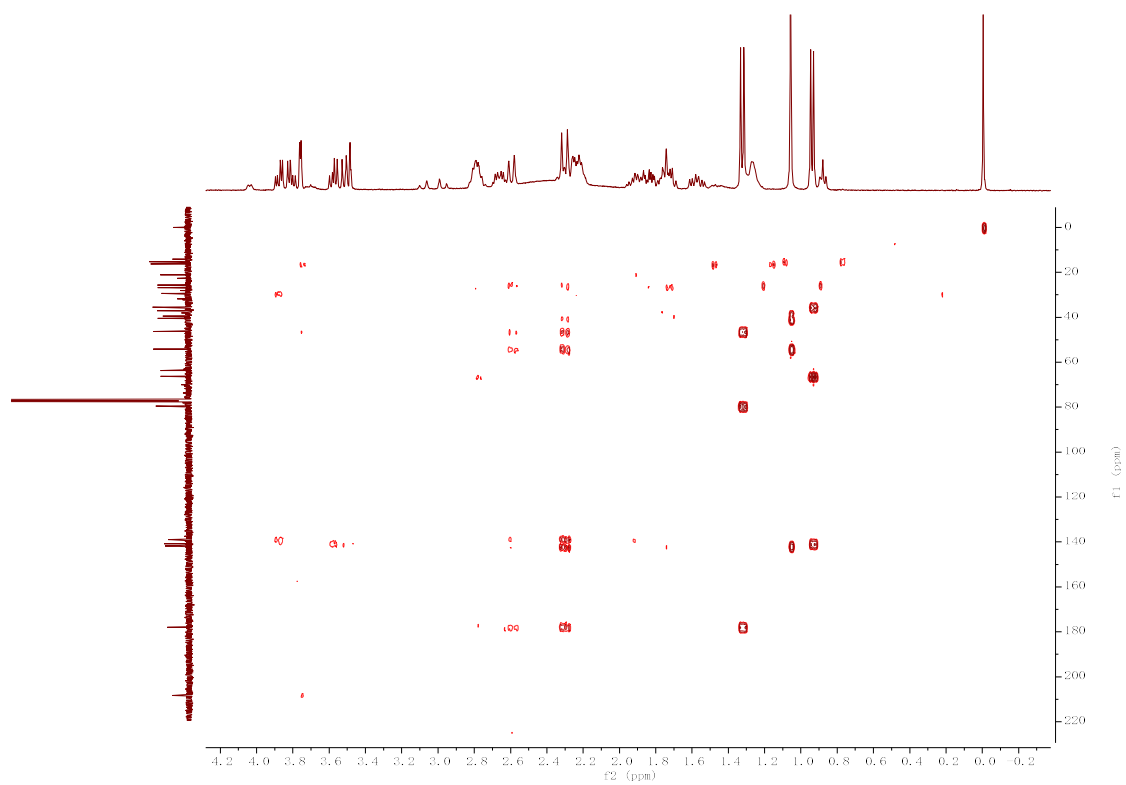


Figure S63. ¹H-¹H COSY spectrum of dongtingnoid G (7) in CDCl₃

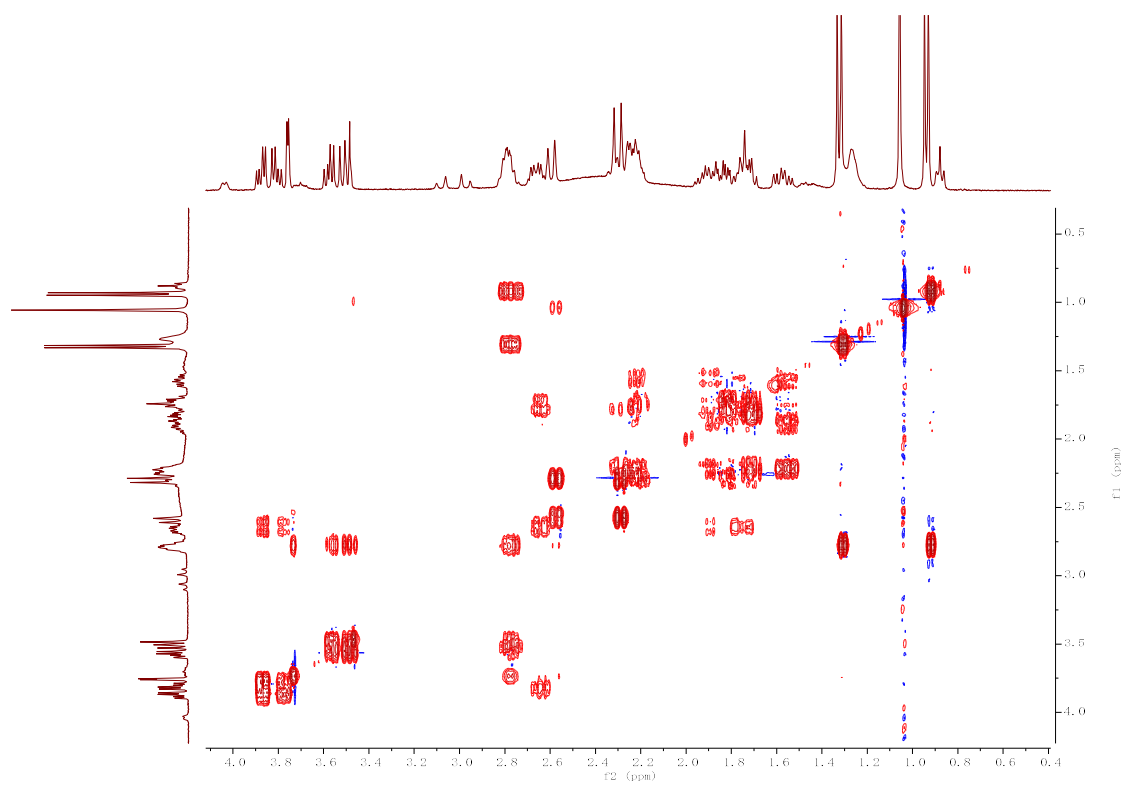


Figure S64. NOESY spectrum of dongtingnoid G (**7**) in CDCl₃

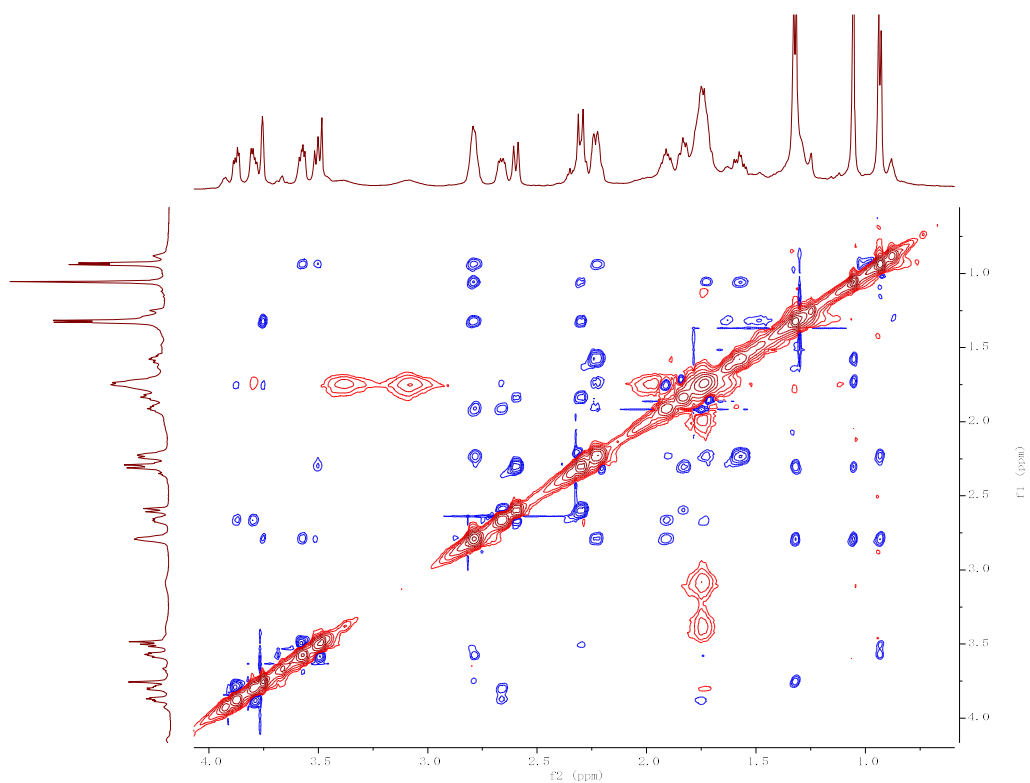


Figure S65. IR spectrum of dongtingnoid G (**7**)

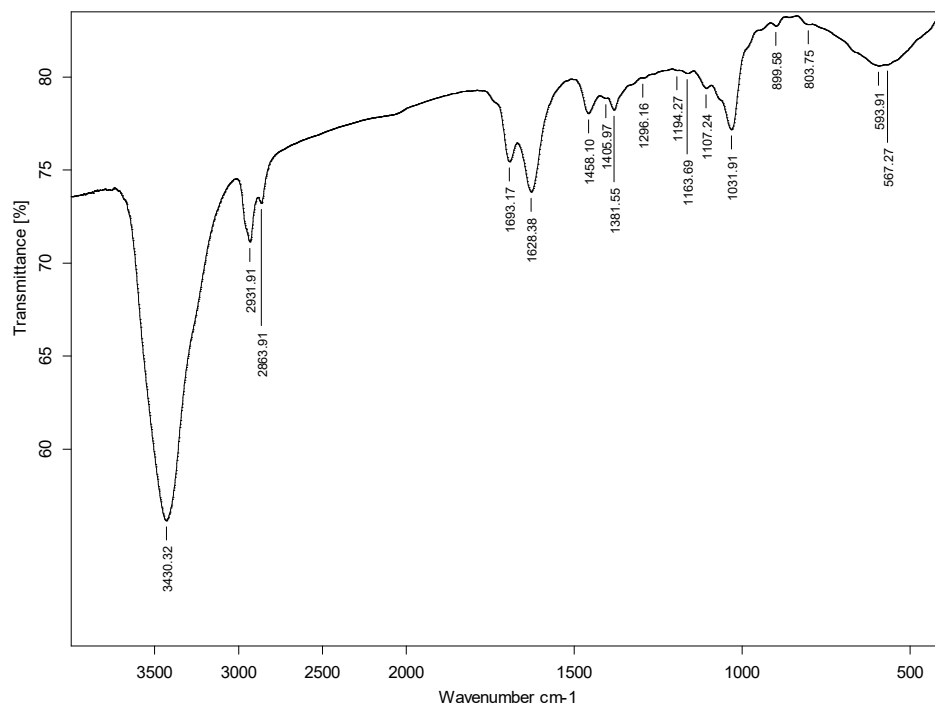
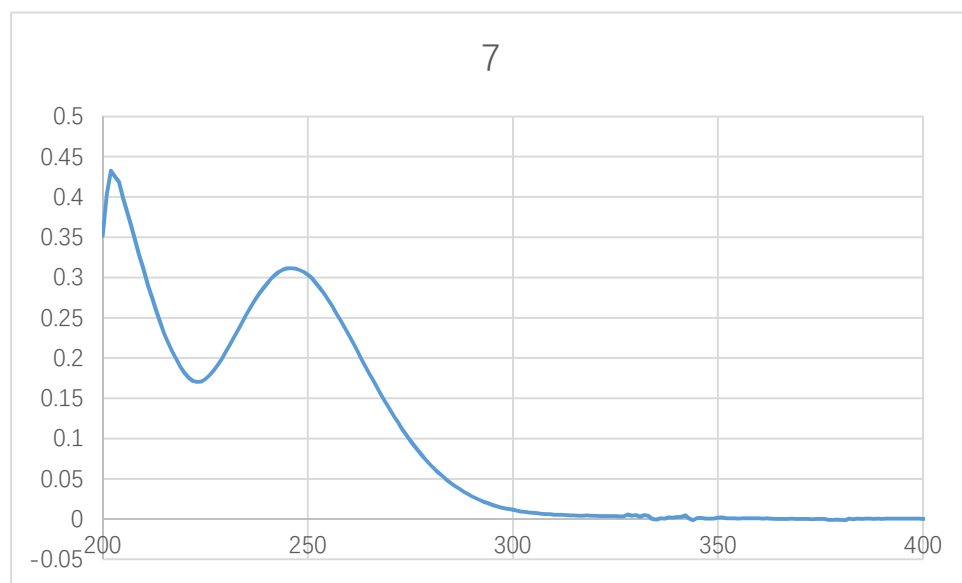


Figure S66. UV spectrum of dongtingnoid G (7)



ECD calculations

The conformations of **3-5** generated by BALLOON^[1, 2] were subjected to semiempirical PM3 quantum mechanical geometry optimizations using the Gaussian 09 program^[3]. Duplicate conformations were identified and removed when the root-mean-square (RMS) distance was less than 0.5 Å for any two geometry-optimized conformations. The remaining conformations were further optimized at the B3LYP/6-31G(d) level in MeOH with the IEFPCM solvation model using Gaussian 09, and the duplicate conformations emerging after these calculations were removed according to the same RMS criteria above. The harmonic vibrational frequencies were calculated to confirm the stability of the final conformers. The electronic circular dichroism (ECD) spectrum were calculated for each conformer using the TDDFT methodology at the B3LYP/6-311++G(d,p)//B3LYP/6-31G(d) level with MeOH as solvent by the IEFPCM solvation model implemented in Gaussian 09 program. The ECD spectra for each conformer were simulated using a Gaussian function with a bandwidth σ of 0.4 eV. The spectra were combined after Boltzmann weighting according to their population contributions and UV correction was applied^[4].

The theoretical calculations of **7** was performed using Gaussian 09^[5]. The 3D structure of **7** was first established based on the NOESY spectra. Its 3D structure was then performed in the SYBYL 8.1 program by using MMFF94s molecular force field. The conformer was optimized using DFT at the B3LYP/6-31+ G(d) level in gas phase. Further optimization at the B3LYP/6-31+G(2d,p) level got the dihedral angles. The optimized conformation was used for the ECD calculations using time dependent Density Functional Theory (TDDFT). The ECD spectra was produced by SpecDis1.6 software^[6]. Then the calculated ECD spectra of **7** was subsequently compared with the experimental ones.

The ECD spectra was simulated by overlapping Gaussian functions for each transition according to

$$\Delta\epsilon(E) = \frac{1}{2.297 \times 10^{-39}} \times \frac{1}{\sqrt{2\pi\sigma}} \sum_i^A \Delta E_i R_i e^{-\left[\frac{(E-E_i)}{2\sigma}\right]^2}$$

Where σ represents the width of the band at $1/e$ height, and ΔE_i and R_i are the excitation energies and rotational strengths for transition i , respectively. $\sigma = 0.30$ eV and R_{vel} had been used in this work.

- [1] M.J.V. And, M.S. Johnson, Generating Conformer Ensembles Using a Multiobjective Genetic Algorithm, *Journal of Chemical Information & Modeling*, 47 (2007) 2462-2474.
- [2] J.S. Puranen, M.J. Vainio, M.S. Johnson, Accurate conformation-dependent molecular electrostatic potentials for high-throughput in silico drug discovery, *Journal of Computational Chemistry*, 31 (2010) 1722-1732.
- [3] G.W.S. Frisch MJT, H. B.; Scuseria, G. E.; Robb, M. A.; Cheeseman, J. R.; Scalmani, G.; Barone, V.; Mennucci, B.; Petersson, G. A.; Nakatsuji, H.; Caricato, M.; Li, X.; Hratchian, H. P.; Izmaylov, A. F.; Bloino, J.; Zheng, G.; Sonnenberg, J. L.; Hada, M.; Ehara, M.; Toyota, K.; Fukuda, R.; Hasegawa, J.; Ishida, M.; Nakajima, T.; Honda, Y.; Kitao, O.; Nakai, H.; Vreven, T.; Montgomery, J. A., Jr.; Peralta, J. E.; Ogliaro, F.; Bearpark, M.; Heyd, J. J.; Brothers, E.; Kudin, K. N.; Staroverov, V. N.; Kobayashi, R.; Normand, J.; Raghavachari, K.; Rendell, A.; Burant, J. C.; Iyengar, S. S.; Tomasi, J.; Cossi, M.; Rega, N.; Millam, N. J.; Klene, M.; Knox, J. E.; Cross, J. B.; Bakken, V.; Adamo, C.; Jaramillo, J.; Gomperts, R.; Stratmann, R. E.; Yazyev, O.; Austin, A. J.; Cammi, R.; Pomelli, C.; Ochterski, J. W.; Martin, R. L.; Morokuma, K.; Zakrzewski, V. G.; Voth, G. A.; Salvador, P.; Dannenberg, J. J.; Dapprich, S.; Daniels, A. D.; Farkas, Ö.; Foresman, J. B.; Ortiz, J. V.; Cioslowski, J.; Fox, D. J., (2009) Gaussian 09, Revision D 01, Gaussian, Inc, Wallingford, CT.
- [4] H.J. Zhu, *Organic Stereochemistry: Experimental and Computational Methods*, Wiley-VCH Verlag GmbH & Co. KGaA, Weinheim, Germany, 2015.
- [5] Gaussian (2010). Gaussian 09: A, electronic structure modeling program. Gaussian Inc., Wallingford CT, USA. URL <http://www.gaussian.com/>.
- [6] SpecDis (2015). SpecDis: A software to process the results of quantum-chemical ECD/UV, ORD, or VCD/IR calculations. University of Wuerzburg, Germany. URL <http://www-organik.chemie.uni-wuerzburg.de/lehrstuehlearbeitskreise/bringmann/specdis/>.